Distribution of Crustal Types in Canada Basin, Arctic Ocean

D. Chian[5*], H.R. Jackson[1], D.R. Hutchinson[2], J.W. Shimeld[1], G.N. Oakey[1], N. Lebedeva-Ivanova[3], Q. Li[1], R.W. Saltus[4], and D.C. Mosher[1]

*corresponding author

[1]Geological Survey of Canada Atlantic, 1 Challenger Dr. Box 1006 Dartmouth, N.S., B2Y 4A2

[2]U.S. Geological Survey, Woods Hole Science Center, 384 Woods Hole Rd., Woods Hole, MA 02543

[3]The Centre for Earth Evolution and Dynamics (CEED), University of Oslo, P.O. Box 1028 Blindern 0315 OSLO Norway

[4]United States Geological Survey, Mail Stop 964, Denver, CO 80225-0046

[5]Chian Consulting, 6238 Regina Terrace, Halifax, N.S., B3H 1N5, deping.chian@gmail.com

Abstract

Seismic velocities determined from 70 sonobuoys widely distributed in Canada Basin were used to discriminate crustal types. Velocities of oceanic layer 3 (6.7 -7.1 km/s), transitional (7.2-7.6 km/s) and continental crust (5.5-6.6 km/s) were used to distinguish crustal types. Potential field data supports the distribution of oceanic crust as a polygon with maximum dimensions of ~340 km (east-west) by ~590 km (north-south) and identification of the ocean-continent boundary (OCB). Paired magnetic anomalies are associated only with crust that has oceanic velocities. Furthermore, the interpreted top of oceanic crust on seismic reflection profiles is more irregular and sometimes shallower than adjacent transitional crust.

The northern segment of the narrow Canada Basin Gravity Low (CBGL), often interpreted as a spreading centre, bisects this zone of oceanic crust and coincides with the location of a prominent valley in seismic reflection profiles. Data coverage near the southern segment of CBGL is sparse. Velocities typical of transitional crust are determined east of it. Extension in this region, close to the inferred pole of rotation, may have been amagmatic. Offshore Alaska is a wide zone of thinned continental crust up to 300 km across. Published longer offset refraction experiments in the Basin confirm the depth to Moho and the lack of oceanic layer 3 velocities. Further north, towards Alpha Ridge and along Northwind Ridge, transitional crust is interpreted to be underplated or intruded by magmatism related to the emplacement of the High Arctic Large Igneous Province (HALIP). Although a rotational plate tectonic model is consistent with the extent of the conjugate magnetic anomalies that occupy only a portion of Canada Basin, it does not explain the asymmetrical configuration of the oceanic crust in the deep water portion of Canada Basin, and the unequal distribution of transitional and continental crust around the basin.

1 Introduction

While most of the world's ocean basins have reliable dates to constrain their tectonic history, the remote and ice-covered Canada Basin in the Arctic Ocean is enigmatic. The lack of clear magnetic anomalies and the paucity of seismic profiles have allowed controversy to flourish on how Canada Basin formed. Hypotheses about the nature of the crust underlying Canada Basin have ranged from oceanization of the continental crust (Shatsky, 1935) to Paleozoic or Cretaceous ocean crust from the Pacific (Churkin and Trexler, 1980) to Mesozoic oceanic crust created through diverse (and often conflicting) opening directions (Lawver and Scotese, 1990; Grantz et al., 2011; Døssing et al., 2013). On-land geological similarities (Embry 1990) and recent detrital zircon studies (Gottlieb et al., 2014) permit

the hypothesis that the Canadian Arctic Islands and northern Alaska were once contiguous but became separated by the seafloor spreading that created Canada Basin. However, the models remain uncertain because of overlaps and inconsistencies in the reconstruction models (e.g., Lawver and Scotese, 1990; Lawver et al., 2002; Lane, 1997; Lane et al., 2015). One way to help resolve conflicts among these many models and reconstructions is to identify crustal types and their distributions within Canada Basin.

Velocity characteristics of rocks can be used to distinguish and map distinct lithologic and crustal types, such as oceanic crust (White et al., 1992). Between 2007 and 2011, Canadian and American collaborators acquired wide angle reflection and refraction seismic data from 152 sonobuoys in the Arctic Ocean primarily to study sedimentary velocities and depths and, where data quality enabled longer source-to-receiver offsets to be analyzed, to also study the deeper basement and crustal components. Of these, 87 sonobuoys are within Canada Basin and 70 are of sufficient quality to be used in this study. Offsets up to 40 km allowed the velocities of crustal arrivals to be measured. In contrast with older studies, the sonobuoy data were acquired with modern GPS navigation and digital recording technology. These seismic data, because of their regional distribution, provide the opportunity for 3D synthesis of velocities and crustal types on a basin-wide scale. This is a major difference from data typically collected on high-resolution 2D transects of continental margins (e.g. Chian et al., 1999; White et al., 2008; Funck et al., 2011). This paper presents the velocity synthesis of crustal layers, particularly the distribution and nature of crustal types based on wide angle reflection/refraction sections, potential field data, and coincident vertical incidence seismic reflection profiles. The newly defined distribution of crustal types adds a new constraint on the formation of Canada Basin.

2 Geological Framework

Canada Basin is a small ocean basin bordered on the south and east by the Alaskan and Beaufort Sea and Canadian Arctic Islands continental margins respectively, on the west by Northwind Ridge of the Chukchi Borderland, and on the north by Alpha Ridge (Fig. 1). The Alaskan, Beaufort and Canadian Arctic Islands margins are sediment covered passive continental margins, although tectonic deformation associated with the northeast extent of the Brooks Range deforms the southeastern Alaskan margin (Helwig et al., 2011; Houseknecht and Bird, 2011). At the southeast corner of the basin, the Mackenzie Delta/fan system extends for ~ 350 km onto the seafloor to ~3800 m water depth. The large structures bounding Canada Basin are diverse. Northwind Ridge is a steep, linear escarpment rising ~2800 m from the abyssal sea floor. The southern edge of Alpha Ridge has irregular and occasionally steep morphology. Between Northwind Ridge and Alpha Ridge lies the Nautilus Basin. Stefansson Basin forms a similar semi-enclosed basin where the Canadian margin joins Alpha Ridge. This paper is restricted to an interpretation of the crust in the region between the northern tip of Northwind Ridge and the Canadian polar margin, south to Alaskan margin (Fig. 1).

The study of passive continental margins is relevant to understanding Canada Basin, because the transition from continental to oceanic crust involves distinct changes in velocity structure, crustal thickness, and reflection character, depending upon whether the passive margin is magma-rich (i.e., volcanic) or magma-poor (i.e., non- volcanic). A schematic cross-section (Fig. 2) shows the main characteristics and distinguishing features of these end member crustal types. Commonly, a transition zone is interpreted to separate oceanic from adjacent crustal types. The nomenclature for this zone has been diverse, ranging from the simple (transition zone, e.g., Whitmarsh et al., 1993; Pickup et al., 1996) to the complex (e.g., multiple domains of Sutra and Manatschal, 2012; Peron-Pinvidic et al., 2013). Along some continental margins, this zone of transition is also sometimes called hyperextended

(Whitmarsh et al., 2001; Sutra and Manatschal, 2012). The work by Lundin and Dore (2011) notes confusion in using the term hyperextension because the term also refers to extended Early Cretaceous rift basins that predate the early Cenozoic breakup of the North Atlantic, i.e., the origin of the hyperextended crust is not necessarily from the final breakup process. Because the analysis in this paper focuses on the extent of oceanic crust, rather than the full transects across the continental margins, and in order to avoid confusion, we use the simplified terminology for thinned continental crust, transitional crust, and oceanic crust (e.g. Chian et al., 1995; Pickup et al., 1996).

Oceanic crust is well known and remarkably consistent in its thickness, lithology, and geochemistry in most of the world's oceans (e.g., White et al., 1992). White et al. (1992) pointed out that one of the triumphs of early marine geophysics was recognizing the oceanic crustal structure being basically the same everywhere. The two crustal layers beneath the sedimentary section have distinct and characteristic velocities: layer 2 has variable velocities (4.5 – 6.6 km/s), a large near-surface velocity gradient (~1.0 /s), and a thickness of ~2.1 km; layer 3 has more consistent velocities (6.7 km/s but no higher than 7.1 km/s), a smaller velocity gradient, and a thickness about twice that of layer 2. Total average thickness of normal oceanic crust for the North Atlantic is 7.08 ± 0.78 km (White et al., 1992). These values are consistent where oceanic spreading rates are greater than 20 mm/yr. Oceanic crust is generally thinner along fracture zones and at slower rates of spreading, where melt is presumed to be limited (Reid and Jackson, 1981; White et al., 1992).

The margins around the southern and central Canada Basin are inferred to be magma-poor (nonvolcanic) passive margins based on the interpreted lack of rift-related volcanic activity in this region (Grantz et al., 1979; Embry and Dixon, 1990; Hall, 1990; Sherwood, 1992; Houseknecht and Bird, 2011). Off the southern Labrador margin, a similar magma-poor margin, the velocity of the continental crust is

5.0-6.6 km/s (Chian et al., 1999). By analogy, the margins around southern Canada Basin are characterized by velocities associated with continental crust or thinned continental crust, i.e., velocities that are no higher than ~6.6 km/s and thicknesses that could range from ~35 to <10 km (Stephenson et al., 1994; Helwig et al., 2011).

In contrast, the northern Canadian polar margin near Alpha Ridge is interpreted as a magma-rich (volcanic) rifted margin having thinned and intruded continental crust underlain by a high velocity layer of 7.5-7.6 km/s interpreted to be volcanic (Funck et al., 2011). Tholeiitic basalt flows and sills broadly distributed across the Arctic are known on Ellesmere, Axel Heiberg, north Greenland and other polar islands (Estrada and Henjes-Kunst, 2004; Tegner et al., 2011; Evenchick et al., 2015). Therefore, the northern Canada Basin might be expected to contain thinned continental crust that changes into a zone with features similar to magma-rich passive margins, i.e., seaward-dipping reflections associated with extrusive subaerial and submarine basalt flows and a high-velocity intruded and underplated lower crustal layer in which velocities are 7.4 km/s or higher but less than upper mantle velocities of ~8.0 km/s (e.g. White et al., 2008).

High velocities are also associated with some magma-poor continental margins where serpentinized upper mantle directly underlies the post-rift sedimentary section (Whitmarsh et al., 1993; 2001; Chian et al., 1995; Pickup et al., 1996), similar to results off Iberia (e.g., Whitmarsh et al., 2000). This zone has refraction velocities of 4.5-7.0 km/s from a 2-4 km thick upper layer overlying a lower layer with a velocity of up to 7.6 km/s. These velocity models provide the analogs for which the velocities measured in Canada Basin can be associated with different crustal types.

3 Methods

3.1 Data acquisition and processing

The sound source for the wide angle reflection/refraction data was an airgun array consisting of 2x500 and 1x150 in^3 Sercel™ G-guns totaling 1150 in^3. The airgun array was fired at a 14-20 s interval for an average trace spacing of 20-30 m. The receivers were Ultrasonic ™ expendable sonobuoys with a single hydrophone deployed at 60 m depth (or occasionally at 300 m depth). The seismic impulses were radio telemetered back to the stacked Yagei™ array on the ship. The sonobuoy signals were digitized onboard ship and stored in SEGY format (e.g. Mosher et al., 2013). All sonobuoy profiles and their interpretations are documented in an atlas (Chian and Lebedeva-Ivanova, 2015).

Expendable sonobuoys do not have internal navigation systems; only the deployment position is known. The direct arrival time used a water velocity profile for the sonobuoy hydrophone at 60 m depth (Lebedeva-Ivanova and Lizaralde, 2011) to calculate the source to receiver offsets. Data processing of sonobuoy wide angle reflection/refraction profiles includes a static time correction for airgun delay, digitizing arrival time T (sec) of direct water wave for all traces, and assigning offsets (Chian and Lebedeva-Ivanova, 2015). The refractions recorded in the sonobuoys traveled nearly horizontally in corresponding layers, producing direct evidence for velocity measurements in sedimentary layers and below. Nearly all sonobuoys in the central and southern Canada Basin had up to a dozen refractions observed at source-receiver offsets of 9-40 km. Since recordings spanned a wide range of frequencies, final modeling used seismic data filtered at 2-50Hz (in some cases non-filtered).

3.2 Modeling procedures

Forward modeling was accomplished using the RAYINVR program (Zelt and Smith 1992, Zelt and Forsyth 1994) and the in-house software of SeisWide (Chian and Lebedeva-Ivanova, 2015). Both the sonobuoy

data and its coincident reflection profile (Chian and Lebedeva-Ivanova, 2015) were first geometrically aligned in distance trace by trace. Major horizons on the reflection profile were digitized to generate a preliminary model in the time domain. Each layer's velocity (V) and gradient should in general match the corresponding refraction slope of the sonobuoy wide-angle data by V = dX/dT, which can be easily measured. This time-domain model was converted to depth for raytracing using RAYINVR, and the resulting travel-time curves were compared to the observed phases on the sonobuoy data. Such comparison was greatly enhanced with NMO-reduced sonobuoy data (Chian and Lebedeva-Ivanova, 2015), especially when coincident reflection profile were available. The NMO-reduction aimed to transform the data such that each wide-angle reflected phase at zero–offset matched exactly with the reflection data. We found that, at the resolution of our experiment, whenever refracted phases were properly modeled, we saw nearly perfect modeling for the corresponding wide-angle reflections. For layers on reflection profile that were not associated with any sonobuoy refractions, a greater vertical velocity gradient usually existed, which were modelled by matching the curvatures of the corresponding sonobuoy wide-angle reflections. In general, a few perturbations of a layer velocity were usually sufficient to arrive at a satisfactory match of the corresponding refraction phase. The process was used for all layers. Since this method worked in the two-way time domain, only perturbations in velocity (not time/depth) were needed because digitized reflection horizons were fixed during the model perturbations. Note that in the sonobuoy profiles, the slopes of crustal refractions at farther offsets can be easily identified where they became first arrivals, not entangled with reverberated and clustered reflective energy. Seismic anisotropy was not considered due to its complexity, lack of sufficient ray coverage in the relatively large study area.

185 **3.3 Error Analysis**

186 Error analysis of the sonobuoy data for 5 main seismic refraction phases and upper mantle reflection
187 phase (PmP) is summarized in Table 1. When picking each phase, every trace that contains visible
188 amplitudes was picked. The calculated uncertainties of the final model depend on the quality of the fit
189 between the calculated and the observed model. Two indicators of the reliability of the model are the
190 number of data points used to constrain the parameters of the layers, and the (root-mean-square) misfit
191 (Trms) between the calculated and observed travel times. Another indicator is the pick error bar of 40-
192 200 ms assigned by visual inspection of the data, which was used to compute the normalized X^2misfit.
193 In general a good fit was achieved partly due to the flat seafloor and low relief on the sedimentary
194 /crustal layers, relatively short offsets (<35-40 km), and the low ray coverage (no rays intersecting each
195 other). Because the sonobuoys do not overlap, the X^2 misfit compiled in Table 1 was better than some
196 other studies using overlapping seismometers such as Funck et al. (2011).

197

198 **Table 1**: *Error analysis of selected sonobuoy velocities in Canada Basin (south of Alpha Ridge Igneous*
199 *Province), based on selected travel-time picks in continental (type 2), oceanic (type 3), and transitional*
200 *(type 4) zones. Type 1 includes other (unassigned) observed upper crustal picks that are used in this*
201 *study. Trms gives the root-mean-square misfit between calculated and picked travel times.*

Crustal Type	Interval Velocity (km/s)	*No. of SBs*	*No. of Picks (total: 18704)*	*Trms (s)*	*Normalized X^2*	*Velocity Error Bound (km/s)*	*Depth Error Bound (km)*
1. Upper (Unassigned)	4.7 ≤ V ≤ 5.4	6	1013	0.045	0.416	±0.2	±0.5
2. Continental	5.5 ≤ V ≤ 6.6	7	1154	0.041	0.259	±0.2	±1.0

3. Oceanic	6.7 ≤ V ≤ 7.1	24	4092	0.035	0.285	±0.2	±1.0
4.Transitional	7.2 ≤ V ≤ 7.6	28	5819	0.036	0.242	±0.2	±0.5
Upper mantle	V ≥ 7.7	13	1619	0.040	0.233	±0.1	±1.0
Moho	(PmP)	22	5007	0.045	0.301		

To estimate the resolution of velocity models, the range of permissible variations in the models was obtained by perturbing velocity values until the computed travel time curves cannot fit the observed phases in both its slope and time. As described in Chian and Lebedeva-Ivanova (2015), the perturbation of layer velocities was done in time domain in which we kept horizons unchanged in time based on coincident reflection profile. For the layer of basement (upper crust in Table 1), the estimated depth error bounds was a combination of errors caused by cumulative velocity errors of all overlying layers, and interpretive (or phase pick) uncertainty on the reflection profiles and on the wide-angle data. Sub-basement resolution estimates (error bounds in Table 1) were all based on wide-angle modeling as, except in very few lines in the north (e.g. Figure 9), reflection data did not penetrate deeper than basement.

3.4 Crustal Classification

Average sedimentary thicknesses throughout Canada Basin are ~4-5 km, and are much greater than thicknesses found above ocean crust in most of the world's oceans (Divins, 2003). In the thickest sedimentary deposits on Alaskan and Beaufort Sea margins, the deepest sedimentary rocks have velocities of 4.7-4.9 km/s. Elsewhere in the basin, the sedimentary velocities generally increase from 1.8-1.9 km/s to 3.5-4.2 km/s at two way travel times of 3-4 s sub-seafloor. The base of the sedimentary section was used as the top of the crust. The top was identified either by a high-impedance reflective unconformity in the coincident multichannel seismic reflection profiles, or by the onset of velocities of

222 ~4.3-5.0 km/s depending on location in Canada Basin. The sedimentary section is described in detail
223 elsewhere (Shimeld et al., 2016).
224
225 Immediately below the flat-lying sedimentary horizons is a layer generally less than 1 km thick that could
226 contain sedimentary as well as crystalline rocks. This layer consists of discontinuous dipping reflections,
227 locally bright continuous reflections containing unconformities, or widely spaced weak reflections. The
228 base of this unit generally forms acoustic basement, typically fading out of diffuse reflections or in
229 places with a distinct reflection. The velocity modeled in this layer is generally in the range of 4.2-4.4
230 km/s. The top of this inferred basement unit is treated as the top of crust and may also represent
231 volcanic rocks interlayered with sedimentary deposits or Proterozoic or Paleozoic sedimentary strata
232 over basement or, in some locations, biogenic deposits. Thus, although the determination of the base of
233 sedimentary section is clear, the onset of the crust has an estimated uncertainty of up to ±0.5 km.
234
235 In order to derive an objective identification of crustal types, five velocity categories were assigned
236 attributes: continental, oceanic, and transitional crusts, as well as two undifferentiated categories
237 representing upper crust and upper mantle (Table 1 and Fig. 3). For oceanic crust there are two
238 exceptions near the spreading center discussed in section 4.1.1. Figure 3 shows the interpretation of
239 crustal types based on velocity. Upper crust and upper mantle velocities were not used in the
240 classification of most of the sonobuoys, exceptions are noted in sections 4.1.3.
241
242 In summary, we characterize thinned continental, transitional and oceanic crust from velocity ranges
243 outlined in Table 1. Each sonobuoy record is assigned a crustal type independently on this basis. In the
244 case where a sonobuoy recorded both continental and transitional velocities, it was categorized as
245 transitional crust, because transitional crust can include thinned continental crust (e.g. Whitmarsh et al.,

1996). For sonobuoys with both oceanic and transitional velocities of 7.3 km/s, other data were used to interpret the crustal type (described in section 4.2.2.). The type categorization is extrapolated away from the sonobuoys locations using coincident seismic reflection profiles and regional potential field data. Finally, the potential field and bathymetry maps are used to assist in interpreting the boundaries of the crustal types.

4 Results

4.1 Sonobuoy data

Of the 87 sonobuoys examined (Fig. 1), 27 were classified as oceanic, slightly more (30) as transitional, and the fewest (13) as thinned continental crust. An additional 17 sonobuoys lacked information about crustal type altogether, either because sedimentary section was too thick for crustal arrivals to be measured (a case where crust is generally too stretched, fractured or broken such as in the Beaufort Sea), noisy traces in the far offsets obscured the deeper arrivals or the recording ended prematurely with no far offsets acquired. The velocity/depth profiles for continental, oceanic and transitional crust are shown in Figures 3a, 3b, and 3c respectively. A sample sonobuoy record from each crustal type is presented in Figures 4, 5, and 6. The sonobuoy names used in this paper are abbreviated from the names listed in the Chian and Lebedeva-Ivanova (2015) atlas, i.e. SB LSL 2010-1 is shortened to SB 1001.

Because of the harsh ice conditions, project objectives and equipment failures, the sonobuoys were not distributed evenly throughout Canada Basin (Fig. 1); the most consistent coverage is in the interior portions of the basin. The continental margin off the Canadian Arctic Islands lacks robust crustal information (only 2 sonobuoys); as well, there is a gap in the coverage where Northwind Ridge meets Alaskan margin. Hence the sonobuoy data set is most representative of the deep-water portions of Canada Basin.

4.1.1 Oceanic Crust (27 sonobuoys)

Roughly thirty percent of the sonobuoys in Canada Basin (i.e. 27) have crustal velocities in the range 6.7-7. 1 km/s, typical of oceanic layer 3 (Fig. 3b). Of these, 12 show mantle refractions (Pn) or less commonly Moho reflections (PmP) with velocities generally of 8.0-8.1 km/s, with a range in velocities of 7.7-8.2 km/s. These mantle arrivals constrain the thickness of oceanic crust to be 5-6 km, somewhat thinner than typical oceanic crust of ~ 7 km (White et al., 1992), and two have crust as thin as 4 km. These thicknesses are consistent with formation in slow spreading mid-ocean ridge settings (Bown and White, 1994). The velocity/depth functions for these sonobuoys (Fig. 3b) favorably compare with those observed in the North Atlantic slow spreading oceanic crust.

SB 0726 (Fig. 4) is representative of data from the oceanic region. The seismic reflection profile (Fig. 4a) shows a change in the amplitude, frequency and continuity of the reflections at the base of the thick flat-lying sedimentary section. The refracted arrivals at the base of this section have been interpreted to have a velocity of 4.4 km/s. Beneath this layer a velocity of 4.7 km/s is observed. This layer could represent the upper part of oceanic layer 2 and might be composed of basalt flows intermixed with sedimentary deposits. Refractions with velocities of between 5.4 and 6.3 km/s are associated with the upper layers of the crust. The above velocities are measured at the top of the layers and have high velocity gradients typical of oceanic layer 2. A clear 6.9 km/s first arrival is observed over a 25-32 km offset (Fig. 4b). At offsets of 33-39 km, a refraction with a velocity of 8.2 km/s (Pn) is observed as the first arrival. Crustal thickness is about 5.5 km.

In the central Canada Basin, the majority of the sonobuoys results indicate oceanic crust. However, SB 0804 and SB 0805 do not show well developed layer 3 velocities (6.7-7.1 km/s) in the middle of the

oceanic region (Figs. 1 and 7). The crustal velocities determined for these two sonobuoys are 6.6 km/s (Fig. 3b) and 7.4 km/s (Fig. 3c) respectively. The 6.6 km/s velocity has an error bar of ±.2 km/s and has been plotted in the oceanic category. The 7.4 km/s velocity requires assigning it to a transitional category. Both of these are located close to the CBGL anomaly (Fig. 8) that has been interpreted to mark the fossil spreading center (Laxon and McAdoo, 1994). Velocity/depth functions lacking layer 3 have been observed in the vicinity of the ultra-slow spreading Gakkel Ridge (Jokat et al., 2003; Jokat and Schmidt-Aursch, 2007; Hermann and Jokat, 2013) and also on the oblique (and ultraslow-spreading) Knipovich Ridge (Kandilarov et al., 2010; Jokat et al., 2012). On the Knipovich Ridge, total crustal thickness is anomalously thin ~3.5-4.0 km and oceanic layer 3 has velocities of 5.7-6.1 km/s and a Pn of 7.-7.5 km/s. Crustal thickness on Knipovich Ridge increases to that more typical of oceanic crust at about 40 km from the ridge axis where the first clear magnetic anomalies are observed. The relatively low velocities in layer 3 are explained by thermal expansion of the young crust, fracturing and serpentinization. White et al. (1992) also points out that in fracture zones, layer 3 is often absent. They suggest the cause for this occurrence in fracture zone is that the melt has migrated laterally away instead of being built up by multiple injections from below. As the spreading ceased at Canada Basin ridge axis, a lack of melt could have also occurred, thus layer 3 would not be well developed and may explain why these two sonobuoys are within the oceanic domain but do not have layer 3 velocities.

4.1.2 Transitional Crust (30 Sonobuoys)

There are 30 sonobuoys classified as transitional crust, with diagnostic velocities of 7.3-7.6 km/s. They are geographically distributed around the oceanic crust (Fig. 1). Of these, 26 have velocities of 7.4-7.5 km/s, and no velocities were higher than 7.5 km/s (Fig. 3c). The original definition of transitional crust has velocities in the range of 4.5-7.0 km/s underlain by velocities of 7.6 km/s that are associated with

serpentinized mantle (e.g. Chian et al., 1995; Pickup et al., 1996). High-amplitude wide angle reflections (PmP) are sometimes observed, providing constraints on crustal thickness.

SB 1034 and the coincident seismic reflection profile (Fig. 5) are representative of data from the transitional crust. The sedimentary section on the coincident vertical incident seismic reflection profile shows a thick section up to 6 km of flat-lying reflectors with a velocity of <=4.5 km/s (Fig. 5a). Beneath the flat-lying horizons, a higher amplitude lower frequency hummocky reflection is observed. The layer beneath this base sedimentary horizon has a 5.3 km/s velocity and a thickness of 2.5 km, based on second arrivals. A clear first arrival refractor with a velocity of 7.4 km/s is observed at the 25-35 km offsets Fig. 5b). This refractor has strong reverberations.

In the southeast part of Canada Basin in the Beaufort Sea, a group of sonobuoys are classified as transitional (Figs. 1 and 3). These sonobuoys (SB 0710, Sb 0711, SB 1025, SB 1026, SB 1027, SB 1031, SB 1032, SB1033 and SB 1034, Fig. 5) have clear 4.3-4.5 km/s first arrivals that break over to 7.4-7.5 km/s. The sedimentary section is greater than 10 km thick. Sedimentary velocities as high as 4.5 km/s and a single well-defined high-velocity layer of 7.5 km/s (e.g. SB 1034) are characteristic of the region. The 7.4-7.5 km/s refractor is sometimes accompanied by a strong reverberatory band of wide angle reflection energy, suggesting that the top of the high-velocity layer may be a sharp boundary. For models to match the curve of the deepest wide angle reflections, masked layers with velocities in the range of 5.4 km/s and 6.2 km/s are required for SB 1027 and SB 1032 respectively (Fig. 3c). It suggests that continental crust of less than a few kilometers thick exists in this region. On SB 1026 (Fig. 3c), the thick sedimentary deposits may rest directly on the 7.5 km/s layer and the crust may be absent.

North of the Alaska margin along Northwind Ridge, velocities interpreted on SB 0722, SB 1013 and SB1014 indicate that thin (continental) crustal layers may also be present (Figs. 1 and 3c). On SB 0722 a 6.1 km/s upper continental crustal velocity lies immediately above the 7.5 km/s layer. Nearby and closer to Northwind Ridge, SB 1013 (Fig.1 and 3c) has well developed base of sedimentary section arrivals and a weak 5.0 km/s refractor overlying a 7.4 km/s event and a possible weak Pn arrival that would limit the depth to Moho to 17 km. SB 1014 to the north of these sonobuoys and adjacent to Northwind Ridge has crustal velocities in the range of, 6.0-6.6 km/s overlying 7.4 km/s. SB 1015 slightly to the east records a 6.3 km/s layer overlying a 7.4 km/s refractor with an associated weak PmP arrival. This velocity range of above 7.4-7.5 km/s is compatible with an earlier result of Jackson et al. (1995) in the same area, suggesting that extremely thin, heterogeneous and possibly continental crust is a common character of this transitional zone in deep water near Northwind Ridge.

4.1.3 Thinned Continental Crust (13 sonobuoys)

Thirteen sonobuoys are classified as thinned continental crust and most have velocities of 5.5-6.6 km/s with no evidence of a higher velocity 7.2-7.6 km/s deep layer (Fig. 3a). Six of these sonobuoys show strong PmP wide angle reflections indicative of an abrupt change in velocity at the crust-mantle interface.

SB 1003 with its coincident reflection profile (Fig. 6), located 260 km north of Alaskan margin, is an example of data displaying continental velocities. On the accompanying seismic reflection record, a thick sedimentary section (>6 km) with horizontal reflections is observed. Arrivals as high as 4.7 km/s (Fig. 6a) are attributed to the sedimentary section based on comparison with the accompanying seismic reflection profile. Basement relief exists with draped high amplitude reflections filling in between these basement highs. Unfortunately, the seismic reflection profile does not have the resolution to determine

whether these highs are rotated fault blocks or merely basement highs. On the sonobuoy record (Fig. 6b), first arrivals of 6.0 km/s are observed over the 20-27 km offsets. A second arrival exhibits a 6.3 km/s event (Fig. 6b and 6b inset). Modeling shows that the rays associated with the 6.0 km/s velocity travel through the layer beneath the deepest sedimentary horizon. Beyond this range another weaker first arrival is discernible with a velocity of 8.0 km/s typical of the upper mantle Pn. Based on the above constraints, the depth to the top of the upper mantle is ~14 km and the crustal thickness is ~4 km or possibly less because the coincident reflection profile shows basement relief of ~1 km.

Offshore of Alaskan margin is the region with the densest concentration of sonobuoys with velocities typical of continental crust: SB 1001, SB 1003 (Fig. 6), SB 1005, SB 1006, SB 1007, and SB 0713, (Figs. 1 and 3). For example on SB1001 (Figs. 1 and 3a), a refraction of 4.9 km/s is observed and interpreted to be continental basement. Wide angle reflections beneath this layer indicate velocities in the range of 5.1-5.4 km/s above the clear PmP. SB 0713 and SB 1003, respectively located about 300 km and 265 km north of the 2000 m contour have thinner sedimentary layers and stronger crustal events. Hence, continental crust is interpreted to extend well into the deep-water portion of Canada Basin off this part of Alaska. However, on sonobuoys nearest the margin due to the thick sedimentary section, many of the crustal arrivals are weak and the sedimentary basement layer is obscured by the multiple.

In contrast, the area offshore of the Mackenzie Delta has only two sonobuoys (SB 1028 and SB 1030) (Figs. 1 and 3a) that have been interpreted to have continental velocities. On SB 1028 refractions with velocities of 5.5 and 6.6km/s are measured. On SB 1030 no crustal refractions are observed but wide angle reflections from the crust exist together with a clear PmP. In order to match the curve of the crustal reflections and PmP arrivals, a masked layer with a velocity of 6.2-6.4 km/s is required for the crust. This velocity is within the range of continental crustal velocities measured by Stephenson et al.

(1994) on the southeastern Beaufort Sea continental margin. Therefore, this area of thinned continental crust is constrained to be much closer to the coast than is the case further west offshore Alaska.

In the northern Canada Basin along the Canadian Arctic Islands, only two sonobuoys are classified as continental, although the data coverage is sparse. SB 0928-1 (Figs. 1 and 3a) is located in a unique, high-relief basement depression about 130 km across (Fig. 8), interpreted as a graben structure (Hutchinson et al., 2012). This sonobuoy is in deep water ~250 km seaward of the 2500 m contour, indicating thinned continental crust here, similar to offshore Alaska, may extend significantly offshore. Offshore of southern Prince Patrick Island, SB 1020 (Fig. 1) has a complex sedimentary section with low velocity zones (Chian and Lebedeva-Ivanova, 2015). An arrival of 6.6 km/s is consistent with the presence of thin continental crust (Fig. 3c).

Two sonobuoys with continental crust are also seen near the northern end of Northwind Ridge. SB 0815 is in shallow water on the ridge has a 5.0 km/s arrival and a poorly resolved 6.0 km/s event. SB 0933-1 has several crustal velocities ranging from 4.4 to 6.6 km/s and is located near its northern tip. These sonobuoys velocities are consistent with the interpretation based on geological sampling that Northwind Ridge is a continental fragment (Brumley et al., 2015).

Upper mantle refractions (Pn) are observed on SB 1003, SB 0713 and SB 0928 with continental affinities. The Pn arrival on SB 1003 and the nearby SB 0713 constrains crustal thickness to 3-4 km and 6 km respectively. The crustal thickness on SB 0928-1 located in the northern portion of Canada Basin offshore of the Canadian Arctic Islands is 7 km. Strong PmP reflections are observed on several of the other continental sonobuoys (SB 1010, SB 1003, SB 1005, SB 1006, and SB 1007) and are indicative of a

411 sharp boundary at the Moho (e.g. Stein and Wysession, 2003). With estimates of crustal thickness in the
412 range of ~3-5 km and Moho depths of 11-16 km, this continental crust is therefore extremely thinned.
413
414 **4.2 Integration with Potential Field Maps**
415 The widely spaced sonobuoys and reflection profiles provide general constraints on the distribution of
416 oceanic, transitional and continental crust. Maps of magnetic and gravity anomalies (Fig. 7 and 8)
417 provide independent data types to further define the spatial distribution of the crustal types. The
418 oceanic polygon is then compared with the potential field data. The circum-Arctic magnetic anomaly
419 map (Gaina et al., 2014) shows that Canada Basin has muted magnetic anomalies compared with the
420 large amplitude magnetic anomalies associated with Alpha Ridge just to the north of it (Fig. 7, Saltus et
421 al., 2011). In the central Canada Basin, the region with linear conjugate magnetic anomalies (Fig. 7) has
422 been interpreted as evidence of seafloor spreading (e.g. Vogt et al., 1982; Grantz et al., 2011).
423
424 The Free air gravity map of Canada Basin (Fig. 8) derived from Andersen et al., (2010) is dominated by
425 large amplitude shelf-edge paired positive-negative gravity anomalies along the edges of Canada Basin
426 that range from 50-150 mGals (Stephenson et al., 1994). An important but smaller scale feature is the
427 narrow low amplitude negative gravity anomaly, the Canada Basin Gravity Low (CBGL), that stretches
428 from the Mackenzie Delta area to the northeast of Canada Basin (Fig. 8). The CBGL has two parts, a
429 southern segment that extends towards the Beaufort Sea, and a northern part, which bisects the
430 oceanic domain polygon, consistent with its earlier interpretation as the location of the fossil ridge axis
431 (Laxon and McAdoo, 1994). The change in direction between the northern and southern segments of
432 the CBGL occurs about 150 km south of the edge of the oceanic domain. Although the geometry of the
433 northern segment of the CBGL can be associated with basement topography and an axial valley in the

oceanic domain, neither our sonobuoy nor our reflection data are of sufficient resolution to determine the character of the basement on the southern segment of the CBGL.

4.2.1 Oceanic Crust

Within the polygon that describes the OCB, the velocity data indicate oceanic crust, sub-parallel linear magnetic anomalies occur (Fig. 7), consistent with the hypothesis that oceanic magnetic anomalies are formed by seafloor spreading (Vine and Matthews, 1963). These linear anomalies have been previously interpreted as evidence of Mesozoic seafloor spreading in Canada Basin (Taylor et al., 1981, Vogt et al., 1982; Grantz et al. 2011). The character of the inner pair of aligned circular highs is similar to those observed over oceanic crust in slow or ultra-slow spreading regimes (Dick et al., 2003, Brozena et al. 2003; Cannat et al., 2006). Visual inspection suggests that the linear magnetic anomalies (Fig. 7) could extend south of the limit of oceanic crustal mapped by velocities. SB 0713 is strategically located for constraining this boundary. The 6.6 km/s velocity that is critical for identifying continental crust is a weak arrival on the sonobuoy record and, combined with our estimated error of ±0.2 km/s, suggest the possibility that it could be interpreted as oceanic crust of a velocity of 6.8 km/s. It is also possible that the high-amplitude magnetic anomalies characterizing the onshore-offshore magnetic D3 domain of Arctic Alaska (Saltus et al., 2011) that is postulated to have thicker and probably stronger lower crust are merging with the oceanic magnetic anomalies and making it difficult to separate the two regions.

The paired conjugate magnetic anomalies fan slightly northward until they reach about 77°N. Northward on the eastern (Canadian Arctic Islands) side of the basin the outer paired anomaly changes direction and the amplitude decreases. The outer magnetic anomaly trends northwesterly and the oceanic crustal domain narrows, consistent with the sonobuoy velocity data (Fig. 7). Northward of the paired oceanic anomalies on the western side of the basin the outer paired magnetic anomaly approaches Northwind

Ridge at an angle. The high amplitude Northwind Ridge Magnetic Anomaly (NoRMA) becomes the dominant magnetic feature. The velocity data are complex in this region near the northern end of Northwind Ridge. There are about 10 sonobuoys displaying the variations: for example on SB 0901-2 a 6.6-6.8 km/s velocity overlies a 7.4 km/s, on SB 0901-3 a 6.4-6.5 km/s velocity overlies a 7.3 km/s layer, and on SB 0901-4 a 6.7-6.8 km/s layer overlies a 7.3km/s event. Oceanic crust, underplating and/or intrusion of magmatic material due to the proximity of the HALIP (Maher, 2001; Døssing et al., 2013) are possible causes of the two lower crustal velocities.

4.2.2 Transitional Crust

Lundin and Doré (2011) have pointed out the difficulty of assigning velocities in the range of 7.1 -7.7 km/s to particular rock types and that geological setting is important in assessing their origin. Transitional crust in southern Canada Basin is associated with lower amplitude amorphous magnetic anomalies of variable size and orientation. Some of this pattern may be the result of the great thickness of sedimentary section beneath the Mackenzie fan, depressing both the basement and magnetic source layers, but this pattern could also result from demagnetization of the crust similar to anomalies resulting from serpentinization (Whitmarsh et al., 1993; Bronner et al., 2011). The general similarity of these anomalies with the adjacent continent, particularly the Canadian Arctic Islands (Fig. 7), suggests that at least some of this transitional crust is associated with the rifting processes that preceded formation of oceanic crust in Canada Basin. By analogy with Iberia (Whitmarsh et al., 2001), we favor the interpretation that this area of transitional crust is serpentinized mantle underlying extremely thinned continental crust.

In contrast, an elongate high-amplitude magnetic anomaly (NoRMA) dominates the transitional crust subparallel to and just east of Northwind Ridge in the western and northwestern Canada Basin. This

intense anomaly is considered part of Alpha Ridge magmatic zone (Saltus et al., 2011), the 7.3-7.7 km/s velocities may be due to the emplacement of magmatic material related to Alpha Ridge (Døssing et al., 2013). The actual velocity measured on 4 sonobuoys (SB 0812, SB 0813, SB 0901-3, and SB 1016) near the northern tip of Northwind Ridge is 7.3 km/s and on SB 1017 a velocity of between 7.2 and 7.4 km/s is noted. P-wave velocities of 7.3 km/s are unique to this region and their implications are discussed in section 5.5.

4.2.3 Thinned Continental Crust

The area of thinned continental crust in southern Canada Basin, near Alaskan margin, is another region where the magnetic data are helpful in refining crustal type. Saltus et al. (2011) defined a broad positive magnetic anomaly D3 in Alaska that could extend offshore (Fig. 7) and roughly encompass the area of thinned continental crust, as defined by lower crustal velocities ≤6.6 km/s. The offshore portion of the D3 domain may be a structurally competent continental crustal block that resisted breaking apart during the rifting process.

4.3 Seismic Transects

Coincident seismic reflection profiles provide the opportunity to compare the reflection characteristics with crustal types inferred from sonobuoy velocity classifications and potential field data to better understand the tectonic setting of Canada Basin. Here we use depth to basement, basement topography and reflectivity to further refine our interpretations of crustal domains. Four transects (Figs. 9-12) in Canada Basin (Figs. 1, 7, 8) illustrate oceanic crust and the adjacent crustal domains.

4.3.1 North Canada Basin Transect (Fig. 9)

505 The composite profile across north Canada Basin (Fig. 9) reaches from near the northern tip of
506 Northwind Ridge to the adjacent margin offshore of northern Prince Patrick Island (Figs. 1, 7, 8). The
507 sedimentary section is generally less than 4 km thick along this transect. Oceanic crust that meets our
508 simple velocity criteria is at its narrowest width, about 150 km, and mostly consists of a deep valley and
509 the adjacent basement highs. The shape of the valley is well defined, similar to the valley on slow- and
510 ultra-slow spreading mid-ocean ridge segments (Dick et al., 2003; Ehlers and Jokat, 2009). Its position
511 coincides with the position of the CBGL, adding an important detail in support of the interpretation that
512 the CBGL represents a fossil spreading center (Laxon and McAdoo, 1994). The sedimentary deposits in
513 the valley are at least 1 km thicker than the surrounding deposits. Our interpretation of the seismic
514 section is that this is a fossil spreading center with axial valley and rift shoulders.
515
516 The top of transitional crust at the western boundary of the oceanic domain is ~1 km deeper than the
517 rift shoulder and is highly reflective. The bright reflection (Fig. 9b inset) package (Fig. 9b and c) is offset
518 by as much as 0.5 sec in many places, as if faulted, as it rises towards Northwind Ridge. Velocities within
519 this highly reflective unit (4.4-5.6 km/s) are consistent with the presence of basaltic flows, in which the
520 offsets are either due to faulting or they were emplaced on a faulted surface. Seaward dipping
521 reflections (SDRs) are also observed. On SB 1017 on the reflection line that obliquely crosses this
522 transect, a 6.2 km/s is underlain by a 7.2 km/s velocity that indicates transitional crust. However on SB
523 0901-4, just to the north of the seismic transect, a velocity 6.8-7.0 km/s typical of layer 3 is observed on
524 the OCB. Lower crust velocities of 7.2-7.4 km/s are also observed, which is the basis for interpreting this
525 crust as transitional crust. However this region could be oceanic crust with additional high velocity
526 magmatic material from the adjacent Alpha Ridge. Near where the transect crosses Northwind Ridge,
527 weathered basalts interpreted to originate from basalt flows and shallow water volcaniclastic deposits
528 were dredged in 2008 and 2009 (Mukasa et al., 2009; Brumley et al., 2015). Near and on Northwind

Ridge, velocities of 6.3-6.4 km/s, are interpreted to be continental crustal velocities, which is consistent with Northwind Ridge (as part of the larger Chukchi Borderland) representing a subsided crustal block.

On the eastern side of the transect, a thicker sedimentary section with associated deeper basement (location at SB 0928-1) and irregular depths to basement with abrupt offsets is imaged (Fig. 9b). There is only one seismic profile that crosses this depression but its extent can be traced along a rectangular-shaped negative gravity anomaly approximately 60 km across and 200 km long (Fig. 8). The sub-sedimentary velocity of 6.2 km/s is interpreted as continental. The edges of this deep basin on the gravity map have a northeasterly trend and could be wrench-related if the offsets are interpreted as faults on basement. If the offset bright reflections are related to flows or sill intrusions rather than faulting, the basin may alternatively be a deeply subsided pre-rift basin. The magnetic map (Fig. 7) shows a narrow linear magnetic anomaly in this deep basin, the anomaly is about 20 km across and 80 km long. At the eastern edge of the profile a prominent basement high associated with an ovoid positive magnetic anomaly (Fig. 7) may be a volcanic edifice. If the basement depth were due to extensive stretching and subsequent capping with flows or intrusives, it might compensate for the narrowing of the oceanic crust at the axial valley on this transect.

4.3.2 Central Canada Basin Transect (Fig. 10)

The composite profile across the central part of Canada Basin (Figs. 1, 7, 8) is in a region where sedimentary units are between 4 and 7 km thick. The oceanic crust is about 340 km in width here. The profile illustrates both symmetric and asymmetric features. The symmetry is illustrated by the distinctive low-amplitude, high-relief basement reflection associated with oceanic crust surrounded by high-amplitude, low-relief reflections in the adjacent zones of transitional crust. The asymmetry is related to

552 the shallower depth to base of the sedimentary section on the west near Northwind Ridge in contrast to
553 the east, where a greater sedimentary thickness has presumably depressed basement.
554
555 Oceanic crust is characterized by blocky relief with offsets between 0.5 – 2.0 km. There is little
556 reflectivity below the basement horizon. The position of the CBGL is shown and is associated with a
557 depression in the basement relief at the position of SB 0810. The distribution of oceanic crust is
558 asymmetric about 200 km wide in the eastern portion and 140 km wide in the western section. On the
559 western side of the basin near Northwind Ridge, a lower crustal velocity of 7.4 km/s (i.e., transitional
560 crustal velocities) is observed.
561
562 The base of the sedimentary layer on top of transitional crust (Fig. 10) on either side of the oceanic
563 domain has lower relief and in the west stronger reflectivity for about 0.5 km into the crust. Transitional
564 crust next to oceanic crust is also slightly deeper than the central oceanic basement blocks. Transitional
565 crust at the western end of the profile consists of an upper part that is 5-8 km thick with velocities
566 similar to either continental or upper oceanic crust (5.0-6.6 km/s) and a lower part that is 6-7 km thick
567 with a velocity of 7.4 km/s. On the west, the zone of the transitional crust overlaps with the high-
568 amplitude magnetic anomaly NoRMA (Fig. 7). The transitional velocities of 7.4 km/s have been called
569 high velocity lower crust (HVLC) and associated with underplated magmatic material similar to what
570 would be found along a magma-rich (volcanic) continental margin for the following reasons:(a) the
571 continuity of this anomaly with the magnetic domain of the Alpha Ridge (Saltus et al., 2011), (b) the
572 proximity of dredged basalts on Northwind Ridge (Andronikov et al., 2008; Mukasa et al., 2009), and (c)
573 the local presence of oceanic layer 3 velocities up to 6.8 km/s in the transitional region.
574

On the eastern (Canadian) side of the profile, basement in the narrow transitional crust zone is obscured by the water-bottom multiple; however, where imaged in the multichannel data at its seaward (western) edge, basement relief is subdued and contains bright reflections, similar to the reflectivity patterns of basement near Northwind Ridge. SB 1020 has a thick sedimentary section and an upper crustal velocity of 5.0 km/s. The nearby refraction data of Berry and Barr (1971) (Fig. 1) support the interpretation of continental crust near the margin. The magnetic anomaly at the eastern end of the profile is subdued compared with the western end.

4.3.3 South Canada Basin Transect (Fig. 11)

The southern transect crosses Canada Basin ~300 km south of the central transect (Figs. 1, 7, 8), in a location where the sedimentary section is several kilometers thicker (Fig. 11). Good reflection and refraction control is limited to the region west of the CBGL with SB 1025 and SB 1024 constraining velocities and depths in the thick sedimentary section along the Canadian polar continental margin. Oceanic crust is 160 km wide on either side of the low amplitude CBGL. Basement deepens west of the CBGL, but whether it is a valley cannot be easily determined because of the weak reflections at the basement surface. As in the other transects, the top of oceanic crust is blocky and weakly reflective. The oceanic basement surface is poorly imaged between the CBGL and the Canadian continental margin. At 6-7 km thick (SB 0725, SB 0726), crustal thicknesses are only slightly less than those of typical oceanic crust.

Transitional crustal velocities on this transect are 7.4-7.6 km/s (SB 1013, SB 0723 and SB 0724). On the western edge of the transect (Northwind Ridge), the top of transitional basement has bright reflections (Fig. 11c). A small sub-basin located at SB 1013 could be a synrift structure. Beneath the sedimentary layers, velocities of 4.5-5.2 km/s are interpreted to be highly extended continental crust that is 4-5 km

599 thick above the deep transitional (7.4 km/s) body. This transitional layer is up to 5 km thick (SB 1013)
600 and 225 km wide. The existence of a separate Moho arrival and the location of this body adjacent to
601 Northwind Ridge suggest that this transitional crust is underplated magmatic material. Were it
602 serpentinized upper mantle, the 7.4 km/s event would be the top of upper mantle, nor would one
603 expect strong, clear, separate arrivals for a PmP or Pn. Near SB 0723 and SB 0724, velocities in the upper
604 mantle are not well enough constrained to determine whether the transitional body actually thins
605 towards oceanic crust, although the top of the transitional body does deepen from ~12 km at SB 1013 to
606 ~14 km at SB 0724. A sonobuoy on the eastern, Canadian margin (SB 1024) yields sedimentary velocities
607 (4.8 km/s) to a depth of 14 km below the sea surface. The nearest offline SB 1025, approximately 90 km
608 further south, shows a 7.4 km/s event as a strong reverberation at 11-22 km offsets, but only a weak,
609 reverberatory first arrival at offsets of 22-45 km is recorded on SB 1025. There is no indication of a
610 deeper Pn arrival. This transect indicates major differences in crustal thickness, refraction character,
611 and depth between the eastern and western zones of transitional crust. Our preferred interpretation is
612 that transitional crust on the eastern, Canadian margin is serpentinized peridotite.
613
614 4.3.4 North-South Canada Basin Transect (Fig. 12)
615 The final transect crosses the basin from the center of oceanic crust south to Alaskan margin (Fig. 12).
616 This transect is located west of the CBGL (Figs. 1, 7, 8). Oceanic crust in this transect is similar to its
617 character on the central and southern transects, and is a low-amplitude, high-relief reflection. Oceanic
618 layer 3 crustal velocities of 6.9 - 7.0 km/s are first arrivals and well constrained in SB 0726, SB 0727, SB
619 0728. On SB 0804, a 6.6 km/s layer is determined on a weakly defined refraction (Chian and Lebedeva-
620 Ivanova, 2015). SB 0805 is projected into the transect to show sedimentary velocities, but is in the fossil
621 spreading center within the CBGL anomaly and has a transitional crust velocity (7.4 km/s), similar to
622 other velocities measured in slow and ultra-slow spreading centers (Jokat et al., 2003; Jokat et al., 2012).

A 50 km wide zone of transitional crust is adjacent to oceanic crust (SB 1004, Fig. 12), defined by a strong 7.5 km/s refraction. About 10 km to the northwest of SB 1004, SB 0715 has a transitional crustal velocity of 7.4 km/s, confirming the presence of this narrow strip of transitional crust. This is the narrowest transition zone measured in the basin.

Along Alaskan margin, sedimentary strata are up to 10 km thick and are constrained by the presence of subhorizontal, subparallel reflections down to the first multiple reflection and by velocities (Fig. 12) that are as much as 4.7 -4.9 km/s (SB 1007, SB 1006, and SB 1005). On the basis of observed crustal velocities that are typical of continental crust (5.0- 6.4 km/s), crustal thicknesses less than 5 km, and wide-angle arrivals modelled with upper mantle velocities of 8.0 - 8.1 km/s (i.e., precluding the presence of oceanic or transitional velocities), this 180-km wide region is interpreted as thinned continental crust.

In summary, the reflection data add to the picture of the different crustal zones. The top of oceanic crust is typically a weak reflection of high relief compared to the strongly reflective and lower relief at the base of the sedimentary section in the transitional zone. A depression or valley is associated with the CBGL, consistent with the interpretation that it represents a fossil spreading center (Laxon and McAdoo, 1994) with a central rift valley, typical of slow-spreading to ultra-slow spreading ridges (Dick et al., 2003, Jokat et al., 2003). In general, large blocks with offsets up to 2 km define the morphology of oceanic crust, which is much better imaged west of the CBGL. The edges of the transitional crust, while clear on the reflection seismic data where transitional and oceanic crust meet, are not well constrained along the continental margins where transitional and extended continental crust meet. This is mostly because of insufficient data coverage.

Continental crust along the Alaskan and Canadian Beaufort margins is not often imaged in the seismic reflection data because of interference from the water bottom multiple. Where velocities do not indicate oceanic or transitional crust, continental crust is highly extended and often less than 5-10 km thick. Sonobuoys at the north end of Northwind Ridge confirm its origin as a submerged continental block. Another possible continental block is buried beneath the northeast Canada Basin (Fig. 9) where a large graben structure exists.

5 Discussion

5.1 Comparison with published long offset wide angle reflection/refraction data

Several previous regional crustal refraction experiments in Canada Basin (Fig. 1) with offsets of up to 200 km (e.g. Mair and Lyons 1981) provide an important comparison with our more detailed but shorter offset sonobuoy data, especially in determining the velocities and depths of the lower crust and mantle.

5.1.1 Near Alaskan margin

Near the central Alaskan margin in southern Canada Basin (Figs. 1 and 13), Mair and Lyons (1981) used sparsely spaced explosive shots on a cross array and recorded clear refractions. The primary velocities measured were a 4.3 km/s arrival, a weaker event of 6.6 km/s with a low gradient and a better defined 7.5-7.7 km/s layer with a high gradient increasing to 8.1-8.4 km/s out to a range of 200 km. Their velocity model is projected onto our adjacent line in Figure 13 with sonobuoys measurements and reflection profiles. Their velocities of 4.3-4.5 km/s were interpreted as representing oceanic layer 2. The 4.4-4.6 km/s velocities that we measure can be compared to our coincident reflection profiles where a thick sedimentary section is observed. Without access to reflection profiles, they assumed that these velocities represented oceanic layer 2.

Beneath this layer they interpreted only a few first arrivals in the 20-40 km range to constrain the 6.6-6.8 km/s velocity. However, the geometry of their cross array shows this layer thickens towards the margin and has a low gradient. On SB 1002 near the Mair and Lyons experiment, we observed a 7.5 km/s refraction associated with a strong reflection that requires a continental velocity of 5.0 km/s to model its shape. On SB 1003, the basement refraction velocity of 5.9-6.0 km/s is typical of continental crust and underlies the clear sedimentary section determined from the coincident seismic reflection profile. On nearby SB 1005 (Fig. 12), beneath the sedimentary section, velocities of 4.9, 5.3 and 6.0 km/s are interpreted from a noisy record section. On SB 1006 (Fig. 12), velocities of 5.0-5.3 and 6.0-6.6 km/s are weak and accompanied by a strong PmP. Mair and Lyons (1981) interpreted their 6.6-6.8 km/s as oceanic. The lower velocities on the sonobuoys, the lack of linear magnetic anomalies and the surface characteristics of basement suggest thinned continental crust.

Mair and Lyons (1981) measured a 7.6 km/s velocity consistent with our observations of 7.5 km/s velocities on SB 1002 and SB 1004. Furthermore, they were able to determine that this layer had a high gradient based on their long offset arrivals. They interpreted this layer as either part of oceanic layer 3 or serpentinized peridotite. Oceanic layer 3 does not typically have a high gradient or velocities in the range of 7.5-7.6 km/s but a serpentinized layer does (Christensen, 2004). Therefore in our model (Fig. 13) this layer is interpreted as serpentinized peridotite underlying thinned continental crust consistent with the generalized model of a magma-poor margin (Fig. 2).

The sedimentary section (Fig. 13), as interpreted from the seismic reflection profile and the velocities, thickens from SB 0726 towards the margin. The crustal layer thins from the continental margin towards the centre of the basin where it is underlain by a 7.5-7.6 km/s layer. The transition to oceanic crust (Fig. 13) takes place, not at the shelf break (Mair and Lyons, 1981), but 275 km seaward of the shelf break

695 between SB 1003 and SB 0726. As illustrated on SB 0726, well defined layer 3 velocities of 6.9-7.1 km/s
696 and lineated magnetic anomalies are observed. The broad magnetic anomalies near SB 1006 (the D3
697 zone of Saltus et al., 2011) are gradually replaced by more linear anomalies that continue seaward in the
698 region displaying clear oceanic crustal velocities. The zone where magnetic lineations are observed, but
699 velocities suggest the presence of continental crust, occur at the ocean-continent boundary suggesting
700 that the continental crust has been intruded with basaltic rocks.
701
702 5.1.2 Near southern Northwind Ridge
703 Also in southern Canada Basin, Baggeroer and Falconer (1982) carried out a crustal refraction program
704 near and parallel to SB 1009, SB 1010 and SB 1011 (Figs. 1 and 14). They used two types of receivers, a
705 multichannel hydrophone L-shaped array with 600 m length on each arm and an ocean bottom
706 seismometer. The sound source was 5 explosive charges at offsets from 39 to 73 km. They recorded a
707 very strong event with an estimated velocity of 4.9 km/s arrival and a 7.9 km/s arrival that they
708 interpreted as the Moho. Their experiment was located only 5 km to the east of one of our reflection
709 profiles and about midway between SB 2009 and SB 2010. SB 1009 and SB 1010 recorded high
710 amplitude 4.5-4.6 km/s arrivals. On SB 1011, weaker but observed velocities of 5.0 and 5.8 km/s are also
711 seen (Chian and Lebedeva-Ivanova, 2015), similar to the 4.9 km/s velocity of Baggeroer and Falconer
712 (1982). A velocity of 7.5 km/s is observed on the sonobuoy data breaking over as a first arrival at about
713 25 km offset. Baggeroer and Falconer (1982) observed a velocity of 7.7 km/s from 39.4 to 73.2 km range
714 with the 4.9 km/s event breaking over to 7.9 km/s event at 29.1 km. The depth to the high velocity layer
715 7.5-7.7 km/s is predicted to be 9.8-10.7 km below the seafloor by Baggeroer and Falconer (1982),
716 consistent with the velocity model for SB 1011.
717

718 The results of both experiments are similar but difficulties in interpreting them remain. The 4.5 km/s
719 arrival on the sonobuoy data, when compared with the coincident reflection profile, occurs within the
720 sedimentary section. It is puzzling why a 4.5-4.9 km/s sedimentary arrival at about 4.3 km depth within
721 a 6 km thick sedimentary section should be so strong a refraction. Baggeroer and Falconer (1982) made
722 an important observation that this event exhibits high attenuation with offset, suggesting a sharp
723 gradient typical of a change at the sedimentary basement interface. They also commented that their 4.9
724 km/s velocity was high for a sedimentary layer and could mean that this layer was compacted
725 sedimentary material. Baggeroer and Falconer (1982) were also concerned that no layer 3 velocities had
726 been measured. Based on spectral analysis of the array data, layer 3 was thin (less than 2 km thick) or
727 absent. The location of their experiment coincides with the region of thinned continental crust
728 extending north from Alaskan margin (SB 1001 to SB 1005). In our more spatially distributed and shot-
729 intensive sonobuoy data, velocity analysis did not reveal a typical layer 3 oceanic velocity. Our favored
730 interpretation is a thick sedimentary section overlying thin continental crust with a velocity of 5.0-5.8
731 km/s, with a measured Moho velocity beneath it.
732
733 Moreover, when our velocities from SB 1009, SB 1010 and SB 1011 are plotted on the coincident
734 reflection profile, our 4.8 km/s arrival on SB 1009 and SB 1010 corresponds with a major change in the
735 reflection profile to lower frequency, less parallel arrivals suggesting the top of basement. The velocity
736 of the crust ranges from 4.8-5.3 km/s consistent with continental velocities with no indication of oceanic
737 layer 3. Near SB 1011 the possible basement horizon changes character (Fig. 14). A series of high
738 amplitude, probably sedimentary, reflections are observed infilling an irregular basement structure. The
739 velocity function for SB 1011 is typical of transitional crust with a 7.5 km/s measurement. Similar
740 topographic irregularities in base of the sedimentary layer and the change to serpentinized crust also

741 occur on the North-South transect (Fig. 12). The magnetic map (Fig. 7) shows a strong positive anomaly
742 in the vicinity of SB 1009 and SB 1010 (Fig. 1) becoming subdued at the location of SB 1011.
743
744 5.1.3 Near the Canadian polar margin
745 Along the northern Canadian margin (Figs. 1 and 10), Berry and Barr (1971) conducted a refraction
746 experiment that had sparse recording and shot intervals. They measured a crustal velocity of 5.4 km/s
747 and a Moho velocity of 8.1 km/s at a poorly resolved depth of 15 ± 9 km mid-way down the continental
748 slope, suggesting thinned continental crust. Two sonobuoys near to, but seaward of the Berry and Barr
749 (1971) refraction line (Fig. 1) provide additional data for the crust in deeper water. SB 1020, slightly
750 south and seaward of the Berry and Barr (1971) line has a well resolved 6.6 km/s layer. The sonobuoy
751 closest to the continental margin, SB 0834, (Fig. 9) recorded data sporadically beyond 17 km offset;
752 however, there were indications of refraction with a 7.4 km/s velocity typical for transitional crust.
753
754 In summary, the earlier refraction experiments in the Canada basement can be put in context with our
755 results. Most of these experiments were along the edges of Canada Basin and did not have coincident
756 reflection profiles making it difficult for the extent of the thick sedimentary deposits to be resolved. The
757 high velocities in the range of 4.5-4.9 km/s in sedimentary section were often interpreted as oceanic
758 layer 2. None of the earlier experiments identified a clear oceanic layer 3 velocity. Based on their
759 distribution in the periphery of Canada Basin, none of them were actually located on oceanic crust. Our
760 more closely sampled sedimentary and upper crustal wide angle reflection/refractions, the magnetic
761 patterns and reflection profiles suggest these experiments actually recorded a sedimentary section
762 overlying transitional or thinned continental crust, consistent with their lack of oceanic velocities.
763
764 **5.2 Constraints on the Opening of Canada Basin**

765 The sonobuoy velocities, seismic reflection profiles and potential field data consistently describe a
766 region of typical and distinctive oceanic crust in Canada Basin (Fig. 15), primarily associated with the
767 northern segment of the CBGL. Our data distribution is insufficient to assign crustal type near and to the
768 west of the southern segment of the CBGL. The paired magnetic anomalies and the general symmetry of
769 oceanic crust around the CBGL, are consistent with the counter clockwise rotation of Alaska with a pole
770 of rotation located in the south of the Beaufort Sea (e.g., Grantz et al., 2011, and included references).
771
772 The combined data sets indicate that the area of oceanic crust is a sub-region of the larger Canada Basin
773 (Fig. 15) and a plate reconstruction must also account for the unknown but finite extension in the
774 transitional crust (e.g., Alvey et al., 2008; Müller et al., 2008). The added space from this more
775 restricted closure might accommodate parts of Northwind Ridge and the Chukchi Borderland, which
776 otherwise require special tectonic accommodation to avoid the overlap with the Canadian Arctic Islands
777 (e.g., Grantz et al., 2011; Brumley et al., 2015). Detrital zircon analysis identify that the Alaska Beaufort
778 margin was in close proximity with the opposing margin of the Canadian Arctic Islands during the
779 Ellesmerian Orogeny into Mesozoic time (Gottlieb et al., 2014). The closure proposed in Gottlieb et al.
780 (2014) results in a 55^{o} rotation, or 10^{o} less than the 66^{o} rotation proposed by Grantz et al. (2011). The
781 width of the southern edge of the polygon of oceanic crust (~340 km wide), puts limits on the amount of
782 rotation, assuming that the rotation is symmetrical around a pole south of the Beaufort Sea. However,
783 the new data presented here and onshore constraints (Lane et al., 2015) indicate that the rotational
784 model does not satisfy all the observations.
785
786 **5.3 Rate and Age of Seafloor Spreading**
787 The thickness and morphology of oceanic crust can augment magnetic anomalies in determining the
788 spreading rate of an ocean basin. Oceanic crustal thicknesses of 4 to 7 km in Canada Basin are typical of

789 slow- spreading rates, i.e., less than full spreading rates of 20 mm/a that produce 6 km thick oceanic
790 crust at average mantle temperatures (Reid and Jackson, 1981; Bown and White, 1994). Faster
791 spreading rates produce average thicknesses of 7.1 km (White et al., 1992).
792
793 The morphology of the axial graben also helps constrain spreading rate (MacDonald, 1982) because
794 slower spreading rates are associated with deeper axial grabens. The depth of the axial graben in
795 Canada Basin based on the seismic reflection data (Fig. 9), is ~1.5 km, consistent with 1.5-3 km depths
796 typical of axial grabens formed by spreading rates of 10-20 mm/a. This depth is greater than the
797 estimate of Grantz et al. (2011), which was based on a single partial crossing of the axial graben. High
798 relief and roughness of the basement surface observed in the multichannel data is also consistent with
799 expected roughness from slow and ultraslow spreading ridges (Malinverno, 1991; Ehlers and Jokat
800 2009).
801
802 Regional geology can help constrain the time of rifting and extension and therefore also places limits on
803 the age of opening. Based on onshore geological constraints such as the dating of onshore rocks
804 assigned to the HALIP, the breakup unconformity, offshore heat flow data and paleomagnetic data on
805 the rotation, seafloor spreading in Canada Basin was estimated to have initiated in the Hauterivian
806 (~134 Ma, Embry and Osadetz, 1988; Embry and Dixon, 1994; Estrada, 2015) and slightly younger
807 offshore of Alaska (Hubbard et al., 1987). The width of the oceanic crust at its southern limit is about
808 320 km from the outside of the paired magnetic anomalies. The outer magnetic anomaly is more
809 continuous than the inner that is formed by a series of small circular highs. This could be due to the
810 magma generation processes slowing down as the spreading center became extinct. Our sonobuoy
811 velocities indicate the crust near the axial valley does not have all the crustal layers observed elsewhere.
812 A slow spreading rate of 20 mm/a would require about 15 Ma to produce this extent of crust. An

ultraslow rate of less than 20 mm/a is not consistent with the development of layer 3 velocities (Jokat et al., 2012).

To correlate the seafloor magnetic anomalies in Canada Basin with the magnetic reversal sequence two linear positive magnetic anomalies with an intervening negative anomaly (Fig. 7) are identified. This reversal sequence cannot happen between ~124 and ~83 Ma due to the long Cretaceous positive polarity chron. Likewise, prior to M5 (~130 Ma), the many short reversals are unlikely to be preserved in a slow spreading ocean basin. Both positive and negative reversals occur in the intervening time interval of ~130 to ~124 Ma (i.e., between M5 and M0). This age is consistent with the Early Cretaceous age of opening based on geological considerations (e.g., Embry and Dixon, 1994).

In order to fit the width of the negative anomaly (i.e. the trough between the two positives) with an assumed spreading rate of 20 mm/a, 5 Ma of time is required. However, the longest negative anomaly duration between M5 and M0 is M3, about 2.3 Ma which would require a higher spreading rate of ~35 mm/a to fit the anomaly. This leaves us with an unresolved problem, that a higher spreading rate (e.g., of 35 mm/a) is required to create the width of the oceanic crust or the time frame is incorrect. If the spreading rate is high, the thickness of oceanic crust should be consistently greater than the observed 4-7 km. A similar identification of magnetic chrons of M4n to M2n (130-127.5 Ma) has been suggested by Grantz et al. (2011). This even more limited age range requires a spreading rate of 75 mm/a that is also inconsistent with anomalously thin oceanic crust measured from sonobuoy velocities. Another possibility is that the paired magnetic anomies are younger. A single whole rock sample from Alpha Ridge was dated using Ar^{40}/Ar^{39} incremental heating with a plateau age of 89±1 Ma (Jokat et al., 2013). The reversal sequence at the end of the long positive chron C34 would be a better fit for a slow spreading ocean. A third possibility is that the magnetic anomalies are due to basement topography.

837

838 **5.4 Seafloor Spreading**

839 The sonobuoy velocity data do not uniquely constrain whether seafloor spreading preceded, coincided
840 with, or followed the magmatism associated with the HALIP. The inferred age of Canada Basin spreading
841 between ~130-~124 Ma closely coincides with onset of magmatism in the HALIP, 130 Ma (Maher, 2001),
842 and revised duration of magmatism in the HALIP of 138-125 Ma (Døssing et al., 2013) or possibly 130-
843 101 Ma (Evenchick et al., 2015). The sparse dates available from onshore dykes that radiate from Alpha
844 Ridge, the offshore segment of the HALIP, suggest basaltic magmatism starting at about 124 Ma
845 (Bleeker et al., 2012; Corfu et al., 2013). The age of bedrock sample from Alpha Ridge 89±1 Ma (Jokat et
846 al., 2013) suggests magmatism on the Alpha Ridge may have had a broad time span. The earliest dates
847 suggest that the creation of oceanic crust in Canada Basin for the region encompassing the northern
848 segment of the CBGL was coeval with initial formation of Alpha Ridge. This timing is probably also the
849 same as formation of the volcanic continental margin at the junction of Alpha Ridge with the Canadian
850 Arctic Islands margin (Funck et al., 2011).

851

852 The age of opening of southern Canada Basin, along the southern segment of the CBGL where it projects
853 ashore near the Mackenzie Delta (Fig. 15), is not well constrained. Transitional crust has not been
854 sampled or dated and is buried by up to 12 km of sedimentary strata beneath the Mackenzie Delta/Fan
855 depositional system (Shimeld et al., 2016). Southern Canada Basin has several characteristics that
856 distinguish it as a separate crustal entity: the more subdued magnetic character, the different
857 orientation of the CBGL relative to the region of oceanic crust further north, the consistently higher
858 sedimentary velocities (Shimeld et al., 2016) and the inferred existence of the oldest sedimentary units
859 along the Beaufort margins (e.g., Hutchinson et al., 2012; Mosher et al., 2013). Extensional basins may
860 have begun forming as early as the Early Jurassic (Hubbard et al., 1987; Embry, 1991; Grantz et al., 1994;

Harrison and Brent, 2005). Whether the transitional crust along the southern segment of the CBGL represents an early (i.e., Jurassic or Early Cretaceous) opening or extension, or is coeval with the formation of oceanic crust requires additional study and modeling.

5.5 The nature of the ocean-continent transition

The border drawn around the ocean crust polygon (Figs. 7, 8, and 15) defines the ocean-continent boundary (OCB), i.e., the location where the seaward edge of transitional crust and the landward edge of oceanic crust meet. The OCB is the most controlled crustal boundary based on our data. It corresponds to the edge of the ocean crust based on the velocity classification (Fig. 3), the edge of the paired linear magnetic anomalies (Fig. 7), and the transition from irregular basement highs on oceanic crust to smoother and, on the eastern, Canadian side, deeper basement on transitional crust on the seismic reflection records (Figs. 9-13).

Outside of the OCB, the seismic data distribution is more widely spaced leading to more uncertainty in characterizing the heterogeneous nature of the ocean continent transition (OCT), i.e., the zone where rapid changes in crustal thickness, lithology, and deformation associated with rifting occurs (Fig. 15). The landward extent of the OCT can be inferred from the integration of the seismic velocity, reflection character, seafloor morphology and potential field anomalies (solid and dashed lines in Fig. 15), but is largely unconstrained from lack of data under the thicker sedimentary cover at the intersection of the Chukchi Borderland with Alaskan margin and along the Canadian Beaufort margins (question marks in Fig. 15a). Nor have we attempted to map transitional crust towards the HALIP as it was mapped by Saltus et al. (2011, white dashed line, Fig. 15). Because of the short hydrophone array necessitated for towing in ice, ice conditions that prevented reaching some parts of the margins, and limits in data collection to water depths generally deeper than 2000 m for cruise objectives, our data are not

positioned to give full crustal transects from continental to oceanic crust. Nor are data sufficient to subdivide the OCT into proximal, distal, necking, coupled, exhumed, or inner and outer zones as defined by other authors (e.g., Peron-Pinvidic et al., 2013; Karner et al., 2012; Sutra and Manatschal, 2012).

The lower crustal velocities used to define the OCT show trends around the OCB. The OCT around the northern extent of oceanic crust has velocities of 7.2-7.3 km/s (described in section 4.2.2). The OCT around the southern extent of oceanic crust has consistently slightly higher velocities of 7.4-7.5 km/s. The only sonobuoy record in southern Canada Basin with a velocity of 7.3 km/s (SB 0709) is very noisy with the direct arrival extrapolated from a weakly constrained wide angle reflection, rather than being based on an observable refraction. The remaining 25 velocity classifications of transitional crust are uniformly 7.4-7.5 km/s. Although these differences are near the limits of resolution of the refraction measurements, their consistency across a large data set suggests the trend of slightly lower velocities in the north and slightly higher velocities in the south is real.

There are good geological explanations for the velocity trends. The 7.2-7.3 km/s slightly lower velocities are consistent with expected velocities from gabbroic melts (e.g. Lundin and Dore, 2011) and highly intruded continental crust such as found off Norway (Mjelde et al., 2005), Hatton-Rockall (Funck et al., 2008), the Canadian volcanic margin at Alpha Ridge (Funck et al., 2011), and southeastern Brazil (Evain et al., 2015). The OCT around the northern extent of oceanic crust is likely to be a magma-rich OCT that is dominated by magmatic intrusion and/or underplating in the lower crust.

The higher velocities of 7.4-7.5 km/s are consistent with velocities interpreted to be serpentinized mantle measured and sampled off the southern Iberia (Whitmarsh et al., 1993; Chian et al., 1999; Dean et al., 2000; Clark et al., 2007). Exhumed and serpentinized continental mantle is one of the dominant

909 characteristics of magma-poor rifting and continental breakup such as documented off Iberia
910 (Whitmarsh et al., 2001; Lavier and Manatschal, 2006; Reston, 2009; Lundin and Dore, 2011). The OCT in
911 this southern area is likely to be representative of a magma-poor OCT that is dominated by
912 serpentinization of exhumed continental mantle.
913
914 A few seismic refraction and reflection criteria exist to help resolve between magma-rich and magma
915 poor settings, and our seismic data locally contain additional information. In a magma-poor setting, one
916 would expect a weak to non-existent Moho arrival because of the gradual change from serpentinized to
917 normal mantle over some depth range (e.g., Chian et al., 1999). In magma-rich setting, the Moho is
918 often a strong and distinct arrival (e.g., White et al., 2008). The offsets used in Canada Basin sonobuoy
919 data are not generally large enough to get robust Pn (Moho) arrivals, but one strong Pn arrival off the
920 Chukchi Borderland (SB 1013, star in Fig. 15) which yields a crustal thickness of 5 km is another
921 supportive piece of evidence that the OCT in that region is magma-rich. This thickness is within the
922 range that might be expected with underplated or intruded magmatic material (Blaich et al., 2011). This
923 Pn measurement and its association with a positive magnetic anomaly that appears to be continuous
924 with Alpha Ridge magnetic domain of Saltus et al. (2011, Fig. 15b) supports the origin of this crust to be
925 a mafic-rich, or underplated/intruded body.
926
927 The crust above the high-velocity lower crust in magma-rich continental margins can have a complex
928 distribution of basalt flows (seaward dipping reflections), sedimentary strata , and variable velocities as
929 well as variable thicknesses along transects (Peron-Pinvidic et al., 2013; Blaich et al., 2011 and
930 references therein). In our Canada Basin data, there are weak seaward dipping reflections in the north
931 (SDR in Fig. 9b), consistent with the magma-rich tectonic setting. Unfortunately, in the eastern and
932 southern (Beaufort) regions, the top of basement is often not imaged by the reflection data because of

933 interference from the water-bottom multiple. Hence the evidence for possible magma-rich features
934 such as seaward dipping reflections in these regions is obscured. Similarly, the small airgun source, the
935 short streamer offsets, and the resulting strong water-bottom multiple also prevent imaging of a
936 possible mid-crustal detachment surface that is often characteristic of magma-poor continental margins
937 (Reston, 2009).
938
939 Moho is also inferred in our dataset from PmP (or reflections from Moho) or occasionally Pn (mantle
940 refractions), in approximately one quarter of the sonobuoys in the OCT. These PmP reflections have
941 strong or intermittent reverberatory arrivals suggesting a relatively sharp, rather than gradational,
942 interface at the top of upper mantle. PmP arrivals are often strong second arrivals at offsets less than 30
943 km and are therefore not affected by degraded signal to noise at more distant offsets. In Canada Basin
944 sonobuoys, the PmP arrivals are distributed around the north, west, and south of oceanic crust. Their
945 distribution about the zone of oceanic crust, similar to the sonobuoys that lack PmP arrivals, suggests
946 that the upper mantle Moho is heterogeneous at the scale of this seismic experiment. This observation
947 does not necessarily eliminate serpentinized upper mantle as an interpretation because the actual
948 velocity measurements of 7.4-7.5 km/s are still diagnostic. However, the number and distribution of
949 PmP arrivals suggest more complexity than the simple gradational velocity model provides. Lacking
950 shear waves, our sonobuoy data cannot be used to calculate Vp/Vs ratios that could perhaps resolve
951 differences between intruded crust and serpentinized mantle (Mjelde et al., 2002).
952
953 A final indicator of the heterogeneous nature of the OCT is its variable width (Fig. 15), which ranges from
954 20 km or less immediately north of Alaska to ~250 km in the vicinity of the Mackenzie delta/fan. The
955 width is ~200 km along the central Chuckchi Borderland and tapers northward towards the HALIP to less
956 than 100 km. It is well known the widths of the OCT on conjugate margins of the North and South

957 Atlantic are asymmetric and variable, and can be narrower than ~50 km or wider than ~200 km (Peron-
958 Pinvidic et al., 2013; Blaich et al., 2011 and references therein). The widths measured around Canada
959 Basin are therefore consistent with measurements and models from other passive margins.
960
961 Two blocks of crust interpreted to have continental crustal velocities abut the two narrowest zones of
962 the OCT, one in the south (Fig. 15; labelled and discussed earlier to coincide with the D3 magnetic
963 domain of Saltus et al., 2011) and one in the north (labelled 78 N, Fig. 15a). Narrow OCTs are often
964 associated with transform margins (Scrutton, 1979), but such an association is not compelling for these
965 regions in Canada Basin. Transform faults are not well developed at ultra-slow spreading ridges such as
966 the Knipovich or Gakkel Ridges in the Arctic) and the magnetic data in Canada Basin do not show offsets
967 that could be interpreted as transforms, either at the locations of these narrow OCTs or elsewhere (Fig.
968 15c). The basement depression at 78^{o}N (Fig. 15) is a steep-sided sedimentary filled basement deep (Fig.
969 9) 80 km by 200 km in extent that is observed in the seismic and potential field data. More detailed
970 investigations to determine the extensional or strike/slip origin would provide important constraints in
971 understanding the development of Canada Basin.
972

973 # 6 Conclusions

974 The most significant result, of the velocity analyses of the broadly geographically distributed sonobuoy
975 data, is that only the central part of Canada Basin is underlain by velocities typical of oceanic crust.
976 When the results of the assignments of velocities to crustal type are superimposed on the magnetic
977 map, we see only the regions with oceanic layer 3 velocities have linear anomalies typical of seafloor
978 spreading. In addition, the CBGL that has been previously attributed to the fossil spreading center
979 bisects the region identified as oceanic crust. Examination of the coincident seismic reflection profiles

shows a deep sediment filled valley that is located along the northern segment of the CBGL. The seismic reflection profiles with coincident oceanic crustal velocities show that the top of seismic basement has high-relief crust and low reflectivity. Velocities determined to be typical of transitional crust are observed on the periphery of the oceanic crust. On the reflection profiles the top of the transitional crust has strong reflectivity and little relief. The magnetic data in the transitional crustal zone have amorphous shaped anomalies. The junction of the oceanic and transitional crust, based primarily on seismic refraction velocities and magnetic character supported by the seismic reflection profiles, is the OCB.

In the Beaufort Sea and further north along the Canadian Arctic Islands (south of the CBGL), velocities typical of serpentinized mantle (7.4-7.5 km/s) are observed in Canada Basin. A serpentinized zone near the margins is a typical feature of slow or oblique spreading oceans. The slow spreading is consistent with the thin oceanic crust (4-7 km thick) and the deep central axis of the fossil spreading center (up to 2 km). In contrast, on the northwestern edge of Canada Basin, seaward of Northwind Ridge in the vicinity of a high-amplitude magnetic anomaly NoRMA, there are several sonobuoys that have velocities in the 7.2-7.3 km/s range. These sonobuoys are also located near the north end of the oceanic zone and close to a region dominated by high amplitude anomalies associated with Alpha Ridge. On this side of Canada Basin, the transitional velocities are interpreted to be typical of a magma rich margin.

Regions of thinned continental crustal velocities of variable thickness are inferred around the edges of Canada Basin. Where identified offshore Alaska and in the northern Canada basin, thinned continental crust occurs in water depths of 3500 m or greater, indicating it reaches far offshore of the continental slope. Published long offset refraction profiles, did not record oceanic layer 3 velocities supporting our interpretation. In the southeastern part of the basin, continental crust extends minimally offshore. The

deep crust at°N basin with a single continental crustal velocity is a distinctive feature on the gravity map. This isolated feature with a significant sedimentary section needs further investigation.

Offshore of the Alaska margin, a broad region with velocities and thickness appropriate for thinned continental crust is predicted from the velocity determinations of the sonobuoy data. Furthermore, the magnetic signature in this region has longer wavelengths than observed elsewhere in Canada Basin and may be an offshore continuation of the broad high-amplitude magnetic anomaly domain (D3) that onshore is associated with thick continental crust, high mafic crustal content, and possibly strong lithosphere.

The most popular hypothesis for the opening of Canada Basin is a counterclockwise rotation of Alaska away from the Canadian Polar margin. The magnetic anomalies in the limited oceanic crust area are consistent with this model. However, although oceanic crust is nearly symmetrically about the CBGL, the asymmetrical distribution of the oceanic crust with respect to the margins indicates that a more complicated plate tectonic model is needed to explain the observed data.

7 Acknowledgements

The officers and crews of the CCGS Louis S. St Laurent and the USCGC Healy are thanked for their tireless efforts in the ice choked waters of the Arctic Ocean in support of the scientific program. The experience, skill and unflagging support of the seagoing technical team lead by Borden Chapman were the key to the success of the program. Funding for this work was provided through the Geological Survey of Canada as part of the Canada's Extended Continental Slope (ECS) Program. This is ESS contribution no. 20150409. Funding for this work was also provided in part through the U.S. Geological Survey as part of the U.S. ECS Project. This article has been peer reviewed and approved for publication consistent with U.S. Geological Survey Fundamental Science Practices (http://pubs.usgs.gov/circ/1367/). Trade names are

used for descriptive purposes only and do not imply endorsement by either the U.S. Geological Survey or the Geological Survey of Canada.

The manuscript was internally reviewed by P. Potter and P. Hart. In addition, this manuscript was improved through critical reviews of V. Childers, W. Jokat and L. Lane.

8 References

Alvey, A., Gaina, C., Kusznir, N.J., and Torsvik, T.H., 2008. Integrated crustal thickness mapping and plate reconstructions for the high Arctic. Earth Planet. Sci. Lett., 274, 310-321.

Andersen, O.B., Knudsen, P., and Berry, P.M.A., 2010. The DNSC08GRA global marine gravity field from double retraced satellite altimetry. J. Geod., 84, 191-199. doi 10.1007/7s00190-009-0355-9.

Andronikov, A.V., Mukasa, S.B., Mayer, L.A., and Brumley, K., 2008. First recovery of Submarine Basalts from the Chukchi Borderland and Alpha-Mendeleev Ridge Region, Arctic Ocean (abs.). AGU Fall Meeting, V41D-2124 (poster).

Baggeroer A., and Falconer, R.H.K., 1982. Array refraction profiles and crustal models of the Canada Basin. J. Geophys. Res., 81, 5461-5476.

Berry, M.J., and Barr, K.G., 1971. A seismic refraction profile across the polar continental shelf of the Queen Elizabeth Islands. Can. J. Earth Sci., 8, 347-360.

Blaich, O.A., Faleide, J.I., and Filippos, T., 2011. Crustal breakup and continent-ocean transition at South Atlantic conjugate margins, J. Geophys. Res., 116, B01402, doi:10.1029/2010JB007686.

Bleeker, W., Kamo, S., Söderlund, U., and Ernst, R.E., 2012. A precise U-Pb baddeleyite age of 121.02±0.25 Ma for a dolerite sill associated with the radiating Queen Elizabeth (Lightfoot River) dyke swarm, Canadian Arctic. Report A107, 12 p., unpublished. In: Ernst, R.E., Bleeker, W., and LIPs reconstruction project team, 2013. Reconstruction of supercontinents back to 2.7 Ga using the Large Igneous Province (LIP) Record: With implications for mineral deposit targeting, hydrocarbon exploration, and Earth system evolution—Year 3 Summary for Project Sponsors. Available upon request to the first author.

1055 Bown, J.W., and White, R.S., 1994. Variation with spreading rate of oceanic crustal thickness and
1056 geochemistry. Earth and Planetary Science Letters, 12, 435-449.

1057 Bronner, A., Sauter, D., Manatschal, G., Peron-Pinvidic, G., and Munschy, M., 2011. Magmatic breakup
1058 as an explanation for magnetic anomalies at magma-poor rifted margins. Nature Geoscience, 4,
1059 549-553.

1060 Brozena, J.M., Childers, V.A., Lawver, L.A., Gahagan, L.M., Forsberg, R., Faleide, J.I., and Eldholm, O.,
1061 2003. New aeromagnetic study of the Eurasia Basin and Lomonosov Ridge: implications for basin
1062 development. Geology, 31, 825-828.

1063 Brumley, K., Miller, E.L., Konstantinou, A., Grove, M., Meisling, K.E., and Mayer, L.A., 2015. First bedrock
1064 samples dredged from submarine outcrops in the Chukchi Borderland, Arctic Ocean. Geosphere,
1065 11 (2): 76-92, (doi.10.1130/GES01044.1).

1066 Cannat, M., Sauter, D., Mendel, V., Ruellan, E., Okino, K., Escartin, J., Combier, V., and Baala, M., 2006.
1067 Modes of seafloor generation at a melt-poor ultraslow-spreading ridge. Geology, 34, 605-608.

1068 Chian, D., Keen, C.E., Reid, I., Louden, K.E., 1995. Evolution of nonvolcanic rifted margins: new results
1069 from the conjugate margins of the Labrador Sea. Geology, 23, 589-592.

1070 Chian, D., and Lebedeva-Ivanova, N., 2015. Atlas of Sonobuoy Velocity Analyses in Canada Basin; Geol.
1071 Survey Can. Open File. 7661: 55p., 1. zip file. doi: 10.4095/295857. http://geoscan.nrcan.gc.ca

1072 Chian, D., Louden, K.E., Minshull, T.A., and Whitmarsh, R.B., 1999. Deep structure of the ocean-
1073 continent transition in the southern Iberia Abyssal Plain from seismic refraction profilers: Ocean
1074 Drilling Program (Legs 149and 173) transect. J. Geophys. Res., 104, 7443-7462.

1075 Christensen, N.K., 2004. Serpentinites, Peridotites, and Seismology: International Geology Review, 46,
1076 795-816.

1077 Churkin, M., and Trexler, J.H. Jr., 1980. Circum-Arctic Plate Accretion – Isolating part of a Pacific Plate to
1078 form the nucleus of the Arctic Basin: Earth Planet. Sci. Lett., 48, 356-362.

1079 Clark, S.A., Sawyer, D.S., Austin, J.A., Christeson, G.L., Nakamura, Y., 2007. Characterizing the Galicia
1080 Bank-Southern Iberia abyssal plain rifted margin segment boundary using multichannel seismic
1081 and ocean bottom seismometer data. J. Geophy. Res., 112, B03408, doi:10.1029/2006JB004581
1082 17 pp.

1083 Corfu, F., Polteau, S., Planke, S., Faleide, J-I., Svensen, H., Zayoncheck, A., and Stolbov., N., 2013. U-Pb
1084 geochronology of Cretaceous magmatism on the Svalbard and Franz Josef Land, Barents Sea
1085 Large Igneous Province, Geology Magazine 150, 1127-1135.
1086 http://dx.doi.org/10.1017/S0016756813000162

1087 Dean, S.M., Minshull, T.A., Whitmarsh, R.B., and Louden, K.E., 2000. Deep structure of the ocean-
1088 continent transition in the southern Iberia Abyssal Plain from seismic refraction profiles: the
1089 IMA-9 transect at 40°20' N. J. Geophy. Res., 105, 5859-5885.

1090 Dick, H.J.B., Lin, J., and Schouten, H., 2003. An ultraslow-spreading class of ocean ridge. Nature, 426,
1091 405-412.

1092 Divins, D.L., 2003. Total Sediment Thickness of the World's Oceans & Marginal Seas, NOAA National
1093 Geophysical Data Center, Boulder, Co.

1094 Døssing, A., Jackson, H. R., Matzka, J., Einarrson, I., Rasmussen, T.M., Olesen, A.V., and Brozena, J.M.
1095 2013. On the origin of the Amerasia Basin and the High Arctic Large Igneous Province – Results
1096 of new magnetic data. Earth Planet. Sci. Lett., 363, 219-230.

1097 Ehlers, B-M., and Jokat, W., 2009. Subsidence and crustal roughness of ultra-slow spreading ridges in the
1098 North Atlantic and Arctic Ocean. Geophys. J., 177, 451-462.

1099 Embry A.F., 1990. Geological and geophysical evidence in support of anti-clockwise rotation of northern
1100 Alaska. Geology, 93, 317-329.

1101 Embry, A.F., 1991. Mesozoic history of the Arctic Islands, Chapter 14, In: Trettin H.P. (Ed.), Geology of
1102 the Innuitian Orogen and Arctic Platform of Canada and Greenland: Geological Survey of
1103 Canada, Geology of Canada no. 3, (also Geological Society of America, The Geology of North
1104 America, v. E), 371-433.

1105 Embry, A.F., and Osadetz, K.G., 1988. Stratigraphy and tectonic significance of Cretaceous volcanism in
1106 the Queen Elizabeth Islands, Canadian Arctic Archipelago. Canadian Journal of Earth Sciences,
1107 25, p. 1209-1219.

1108 Embry A.F., and Dixon J., 1990. The breakup unconformity of the Amerasia Basin, Arctic Ocean: evidence
1109 from Arctic Canada. Geological Society of America Bulletin, 102, 1526-1534.

1110 Embry, A., and Dixon, J., 1994. The age of the Amerasia Basin. 1992, International Conference on Arctic
1111 Margins Proceedings, 289-294.

1112 Estrada, S., 2015. Geochemical and Sr-Nd isotope variations within the Cretaceous continental flood –
1113 basalt suites of the Canadian High Arctic, with a focus on the Hassel Formation basalts of
1114 northeast Ellesmere Island. Int. J. Earth Sci., 104, 1981-2005 doi:10.1007/s00531-014-1066-x.

1115 Estrada, S., and Henjes-Kunst, F., 2004. Volcanism in the Canadian High Arctic related to the opening of
1116 the Arctic Ocean. Zeitschrift der Deutschen Geologischen Gesellschaft, 154, 579-603.

1117 Evain, M., Afilhado, A., Rigoti, C., Loureiro, A., Alves, D., Klingelheefer, F., Schnurle, P, Feld, A., Fuck, R.,
1118 Soares, J., Vinivius de Lima, M., Corela, C., Matias, L, Benabdellouahed, M., Baltzer, A., Rabineau,
1119 M, Viana, A., Moulin, M., and Asianian, D., 2015. Deep structure of the Santos Basin-Sao Paulo
1120 Plateau System, SE Brazil: J. Geophys. Res., 120(8), 5401-5431, doi:10.1002/2014JB011561.

1121 Evenchick, C.A., Davis, W.J., Bedard, J.H., Hayward, N., and Friedman, R.M., 2015. Evidence for
1122 protracted High Arctic large igneous province in the central Sverdrup Basin from stratigraphy,
1123 geochronology, and paleodepths of saucer-shaped sills: GSA Bulletin, 127 (9/10), doi:
1124 10.1130B31190.1, 1366-1390.

1125 Funck T., Andersen, M.S., Keser Neish, J., Dahl-Jensen, T., 2008. A refraction seismic transect from the
1126 Faroe Islands to the Hatton-Rockall Basin, J. Geophys. Res., 113, B12405,
1127 doi:10.1029/2008JB005675, 25 pp.

1128 Funck, T., Jackson, H.R., and Shimeld, J., 2011. The crustal structure of the Alpha ridge at the transition
1129 to the Canadian Polar margin: results from a seismic refraction experiment, J. Geophys. Res.,
1130 116, B1201, doi:10,1029/20/2011jb008411,20118.

1131 Gaina, C., Saltus, R., CAMP-GM group, and the CAMP-geology group 2014. Circum-Arctic mapping
1132 project: New magnetic anomalies linked to the geology of the Arctic. ResearchGate, 5.

1133 Gottlieb, E.S., Meisling, K.E., Miller, E.L., and Mull, C.G., 2014. Closing the Canada Basin: Detrital zirxon
1134 geochronology relationships between the North Slope of Arctic Alaska and the Franklinian
1135 mobile belt of Arctic Canada. Geosphere, 10, 1366-1384.

1136 Grantz, A., Eittreim, S., and Dinter, D.A., 1979. Geology and tectonic development of the continental
1137 margin north of Alaska. Tectonophysics, 59, 263-291.

1138 Grantz, A., May, S.D., and Hart, P.E. 1994. Geology of the Arctic continental margin of Alaska. In: Plafker,
1139 G., and Berg, H.C. (Eds.), The Geology of Alaska: Boulder, Colorado, Geological Society of
1140 America, The Geology of North America, v. G-1, 17-48.

1141 Grantz, A., Hart, P.E., and Childers, V.A., 2011. A geology and tectonic development of the Amerasia and
1142 Canada Basins, Arctic Ocean Chapter 50. In: Spencer, A.M., Embry, A.M., Gautier, D.L.,
1143 Stoupakova, A.V., and Sorensen, K. (Eds.), Arctic Petroleum Geology, Geological Society of
1144 London Memoir, v. 35, p. 771-799, doi:10.1144/M35.

1145 Hall J.K., 1990. Chukchi Borderland. In: Grantz, A., Johnson L., and Sweeney, J.F. (Eds.), The Arctic Ocean
1146 Region. Boulder, Geological Society of America, 593-616.

1147 Harrison, J.C., and Brent, T.A., 2005. Basins and fold belts of Prince Patrick Island and adjacent areas,
1148 Canadian Arctic Islands. Geological Survey of Canada Bulletin, 560, 198pp.

1149 Helwig, J., Kumar, N., Emmet, P., and Dinkleman, M.G., 2011. Regional seismic interpretation of crustal
1150 framework, Canadian Arctic passive margin, Beaufort Sea, with comments on petroleum
1151 potential, In: Spencer, A. M., Embry, A. F., Gautier, D. L., Stoupakova, A. V., and Sørensen, K.
1152 (Eds.), Arctic Petroleum Geology: Geological Society, London, Memoir 35, 527–543.

1153 Hermann, T., and Jokat, W., 2013. Crustal structure of the Boreas Basin and the Knipovich Ridge at 76° N
1154 in the North Atlantic, Geophysical Journal International, 193(3), 1399-1414, doi:
1155 10.1093/gji/ggt048.

1156 Houseknecht, D.W., and Bird, K.J., 2011. Geology and petroleum potential of the rifted margins of the
1157 Canada Basin, In: Spencer, A. M., Embry, A. F., Gautier, D. L., Stoupakova, A. V., and Sørensen, K.
1158 (Eds.), Arctic Petroleum Geology. Geological Society, London, Memoirs 3, 509–526.

1159 Hubbard, R.J., Edrich, S.P., and Rattey, R.P., 1987. Geologic evolution and hydrocarbon habitat of the
1160 Arctic Alaska Microplate. Marine and Petroleum Geology, 4, 2-34.

1161 Hutchinson, D.R., Mosher, D., Shimeld, J., Jackson, R., Lebedeva-Ivanova,N. and Chian, D., 2012.
1162 Basement morphology of the Canada Basin, Arctic Ocean: Tromso, Norway, Arctic Frontiers, 23-
1163 27 January, 2012: full presentation at:
1164 http://www.arcticfrontiers.com/index.php?option=com_docman&task=doc_download&gid=68
1165 0&Itemid=389&lang=en

1166 Jackson, H.R., Grantz, A., Reid, I. May, S.D., and Hart, P.E., 1995. Observations of anomalous crust in the
1167 Canada Basin. Earth and Planetary Science Letters, 134, 99-106.

1168 Jokat, W., 2003. Seismic investigations along the western sector of Alpha Ridge Central Arctic Ocean.
1169 Geophys. J. Int., 152, 185–201.

1170 Jokat, W., Ritzmann, O., Schmidt-Aursch, M.C., Drachev, S., Gauger, S., and Snow J., 2003. Geophysical
1171 evidence for reduced melt production on the Arctic ultraslow Gakkel mid-ocean ridge. Nature,
1172 423, 962-965.

1173 Jokat, W., and Schmidt-Aursch,M.C., 2007. Geophysical Characteristics of the ultraslow spreading Gakkel
1174 Ridge, Arctic Ocean. Geopys. J. Int., 168, 983-998.

1175 Jokat, W., Kollofrath, J., Geissler, W., and Jensen, L., 2012. Crustal thickness and earthquake distribution
1176 south of the Logachev Seamount, Knipovich Ridge, Geophysical Research Letters, 39, L08302,
1177 doi:10.1029/2012GL051199.

1178 Jokat, W., Ickrath M., and O'Connor J., 2013. Seismic transect across the Lomonosov and Mendeleev
1179 Ridges: Constraints on the geological evolution of the Amerasia Basin, Arctic Ocean. Geopys.
1180 Res. Lett., 40, 5047–5051.

1181 Kandilarov, A., Landa, H., Mjede, R., Pedersen, R.B., Okino, K., and Murai, Y., 2010. Crustal structure of
1182 the ultra-slow spreading Knipovich Ridge, North Atlantic, along a presumed ridge segment
1183 center. Marine Geophysical Research, 31, 173-195.

1184 Karner, G.D., Johnson, C.A., Mohn, G., and Manatschal, G., 2012. Depositional environments and source
1185 distribution across hyper-extended rifted margins of the North Atlantic: Insights from the Iberia-
1186 Newfoundland margin. Third Conjugate Margins Conference, Dublin, Ireland, 22-24 August,
1187 2012, p. 7-19.

1188 Lane, L., 1997. Canada Basin, Arctic Ocean: Evidence against a rotational origin. Tectonics, 16: 363-387.

1189 Lane, L.S., Gehrels, G.E., and Layer, P.W., 2015. Provenance and paleography of the Neurokpuk
1190 Formation, northwest Laurentia: An integrated synthesis Geological Society of America Bulletin,
1191 v. 128, no.1-2, p.239-257, doi: 10.1130/B31234.1

1192 Lavier, L.L., and Manatschal, G., 2006. A mechanism to thin the continental lithosphere at magma-poor
1193 margins, Nature, 440, doi:10.1038, 324-328.

1194 Lawver L.A., Scotese C.R., 1990. A review of tectonic models for the evolution of Canada Basin. In:
1195 Grantz, A., Johnson, L., and Sweeney, J.F. (Eds.), The Arctic Ocean Region. Boulder, Geological
1196 Society of America, 593-618.

1197 Lawver, L.A., Grantz, A., and Gahagan, L. M., 2002. Plate kinematic evolution of the present Arctic region
1198 since the Ordovician. In: Miller, E. L., Grantz, A., and Klemperer, S. (Eds.), Tectonic Evolution of
1199 the Bering Shelf-Chukchi Sea-Arctic Margin and Adjacent Landmasses. Geological Society of
1200 America, Boulder, CO, Special Papers, 360: 333–358.

1201 Laxon, S., and McAdoo, D., 1994. Arctic Ocean gravity field derived from ERS-1 Satellite Altimetry.
1202 Science, 265, 621-624.

1203 Lebedeva-Ivanova, N., and Lizaralde, D., 2011. An empirical direct-wave travel time equation for Arctic
1204 Sonobuoy data (abs.) ICAM VI, www2.gi.alaska.edu/ICAMIV/Abstracts/Abstracts.htm

1205 Lundin, E.R., and Doré, A.G., 2011. Hyperextension, serpentenization, and weakening: a new paradigm
1206 for rifted margin compressional deformation. Geology, 39, 347-350.doi: 10.1130/G31499.1.

1207 Ludwig, W.F., Nafe, J.E., and Drake, C.L., 1970. Seismic refraction In: Maxwell, A.E. (Ed.), The Sea, v. 4,
1208 53-84, Wiley Interscience, New York.

1209 MacDonald, K.C., 1982. Mid-Ocean Ridges: fine scale tectonic, volcanic and hydrothermal processes
1210 within the plate boundary zone. Annual Review of Earth and Planetary Sciences, 10, 155-190.

1211 Maher, H.D., 2001. Manifestations of the Cretaceous High Arctic Large Igneous Province in Svalbard:
1212 Journal of Geology, 109, 91-104.

1213 Mair, J. A., and Lyons, J.A., 1981. Crustal structure and velocity anisotropy beneath the Beaufort Sea.
1214 Can. J. Earth Sci., 18, 724-741.

1215 Malinverno, A., 1991. Inverse square-root dependence of mid-ocean ridge flank roughness on spreading
1216 rate. Nature, 352, 58–60.

1217 Mjelde, R., Kasahara, J., Shimamura, H., Kamimura, A., Kanazawa, T., Kodaira, S., Raum, T., and Shiobara,
1218 H., 2002. Lower crustal seismic velocity-anomalies; magmatic underplating or serpentinized
1219 peridotite? Evidence from the Voring Margin, NE Atlantic: Mar. Geophys. Res., 23, 169-183.

1220 Mjelde, R., Raum, T., Myhren, B., Shimamura, H., Murai, Y., Takanami, T., Karpuz, R., and Næss, U.,
1221 2005, JGR, Continent-ocean transition on the Vøring Plateau, NE Atlantic, derived from densely
1222 sampled ocean bottom seismometer data. J. Geophys. Res., 110, B05101,
1223 doi:10.1029/2004JB003026.

1224 Mohn, G., Manatschal, G., Beltrando, M., Masini, E., and Kusznir, N., 2012, Necking of continental crust
1225 in magma-poor rifted margins: evidence from the fossil Alpine Tethys margins: Tectonics, 31,
1226 TC1012, doi: 10.1029/2011TC002961, 28 p. Mosher, D., Chapman, C.B., Shimeld, J., Jackson,
1227 H.R., Chian, D., Verhoef, J., Hutchinson, D., Lebedeva -Ivanova, N., and Pedersen, R., 2013. High
1228 Arctic Marine Geophysical Acquisition: The Leading Edge, May, 936-943.

1229 Mukasa, S., Andronikov, A., Mayer, L.A., and Brumley, K., 2009. Submarine basalts from the
1230 Alpha/Mendeleev Ridge and the Chukchi Borderland (abs.) Geochemistry of the intraplate lavas
1231 recovered from the Arctic Ocean. Geochemica et Cosmochimica Acta, 73 (13) Supplement912.

1232 Müller, R.D., Sdrolias, M., Gaina, C., and Roest, W., 2008. Age, spreading rates, and spreading
1233 asymmetry of the world's ocean crust. Geochemistry, Geophysics, and Geosystems, 9, 19 pp.,
1234 Q04006, doi:10.1029/2007GC001743.

1235 Peron-Pinvidic, G., Manatschal, G., and Osmundsen, P.T., 2013. Structural comparison of archetypal
1236 Atlantic rifted margins: A review of observations and concepts. Marine and Petroleum Geology,
1237 43, 21-47.

1238 Pickup, S.L.B., Whitmarsh, R. B., Fowler, C.M.R., and Reston, T.J., 1996. Insight into the nature of the
1239 ocean-continent transition off West Iberia from a deep multichannel seismic reflection profile.
1240 Geology, 24, 1079-1082.

1241 Reid, I., and Jackson, H.R., 1981. Oceanic spreading rate and crustal thickness. Mar. Geophys. Res., 5,
1242 165-172.

1243 Reston, T.J., 2009. The structure, evolution, and symmetry of the magma-poor rifted margins of the
1244 North and Central Atlantic: A synthesis. Tectonophysics, 468, 6-27.

1245 Saltus, R. W., Miller, E.L., Gaina, C., and Brown, P.J., 2011. Regional magnetic domains of the Circum-
1246 Arctic: a framework for geodynamic interpretation. In: Spencer, A. M., Embry, A. F., Gautier,
1247 D.L., Stoupakova, A. V., and Sørensen, K. (Eds.), Arctic Petroleum Geology. Geological Society of
1248 London Memoirs, 35, 49-60, doi:10.1144/M35.4.

1249 Scrutton, R.A., 1979. On sheared passive continental margins. Tectonophysics, 59(1-4), 293-305

1250 Shatsky, N.S., 1935. Tectonics of the Arctic in Geologiya i polyeznye Severa SSSR: Glavsemorputi, v.1
1251 Geologiya, p.149-168 (in Russian).

1252 Sherwood, K.W., 1992, Stratigraphy, structure, and origin of the Franklinian, northeast Chukchi Basin,
1253 Arctic Alaska plate: Proceedings, 1992 International Conference on Arctic Margins, 245-250
1254 (http://www.boem.gov/ICAM92-245/).

1255 Shimeld J., Li Q., Chian, D., Lebedeva-Ivanova, N., Jackson, R., Mosher, D., and Hutchinson, D. 2016.
1256 Seismic velocities within the sedimentary succession of the Canada Basin and southern Alpha-
1257 Mendeleev Ridge, Arctic Ocean: evidence for accelerated porosity reduction? Geophys. J. Int.,
1258 204 (1): 1-20 doi:10.1093/gji/ggv416.

1259 Stein, S., and Wysession, M. 2003. An introduction to Seismology, Earthquakes and Earth Structure.
1260 Blackwell Publishing.

1261 Stephenson, R.A., Coflin, K.C., Lane, L.S, and Deitrich, J.R., 1994. Crustal structure and tectonic of the
1262 southeastern Beaufort Sea continental margin: Tectonics, 13, 389-400.

1263 Sutra, E., and Manatschal, G., 2012. How does the continental crust thin in a hyperextended rifted
1264 margin? Insights from the Iberia margin. Geology, 40, 139-142. doi:10.1130/G32786.1.

1265 Taylor, P.T., Kovacs, L.C., Vogt, P.R., and Johnson, G. L., 1981. Detailed aeromagnetic investigations
1266 in the Arctic Ocean, 2. J. Geophys. Res., 86, 6323-6333.

1267 Tegner, M., Storey, M., Holm, P.M., Thorarinsson, S.B., Zhao, X., Lo, C.-H., and Knudsen, M.F., 2011.
1268 Magmatism and Eurekan deformation in the High Arctic Large Igneous Province: 40AR-39Ar
1269 age of Kap Washington Group volcanics, North Greenland: Earth and Planetary Science
1270 Letters, 303, 203-214.

1271 Vine, F. J., and Matthews, D. H. 1963. Magnetic anomalies over oceanic ridges. Nature, 199 (4897): 947–
1272 949.

1273 Vogt, P.R., Taylor, P.T., Kovacs, L.C., and Johnson, G.L., 1982. The Canada Basin: Aeromagnetic
1274 constraints on structure and evolution. Tectonophysics, 89, 295-336.

1275 White, R.S., Mackenzie, D., and O'Nions, R.K., 1992. Oceanic crustal thickness from seismic
1276 measurements and rare earth element inversions. J. Geophys. Res., 9, B13, 19,683-19,715.

1277 White, R.S., Smith, L.K., Roberts, A.W., Christie, P.A.F., Kusznir, N.J., and the rest of the iSIMM Team,
1278 2008. Lower-crustal intrusion on the North Atlantic continental margin. Nature, 452, 460-464
1279 doi.10.1038/nature06687.

1280 Whitmarsh, R.B., Pinheiro, L.M., Miles, P.R. Recq, M., and Sibuet, J.-C., 1993. Thin crust at the western
1281 Iberian ocean-continent transition and ophiolites. Tectonics, 12(5), 1230-1239.

1282 Whitmarsh, R.B., White, R. S., Horsefiled, S.J., Sibuet, J-C, Recq, M. and Louvel, V., 1996. The continent-
1283 ocean boundary off the western continental margin of Iberia: Crustal structure of west of Galicia
1284 Bank. J. Geophys. Res., 101, B12, 28,291-28,314.

1285 Whitmarsh, R.B., Dean, S.M., Minshull, T.A., and Tompkins, M., 2000. Tectonic implications of exposure
1286 of lower continental crust beneath the Iberia Abyssal Plain, Northeast Atlantic Ocean;
1287 geophysical evidence. Tectonics, 19(5), 919-942.

1288 Whitmarsh, R., Manatschai, G., and Minshull, T.A., 2001. Evolution of magma –poor continental margins
1289 from rifting to sea floor spreading. Nature, 413, 150-54.

1290 Zelt, C.A., and Smith, R.B., 1992. Seismic travel time inversion for 2_D crustal structure, Geophysical
1291 Journal International, 10, 16-34, doi:10.1111/j.1365-264X.1992.tb00836.x.

1292 Zelt, C. A., and Forsyth, D.A., 1994. Modelling wide-angle seismic data for crustal structure: Southeast
1293 Grenville Province. J. Geophys. Res., 99, 11, 687-11.704, doi: 10.1029/93JB02764.
1294

9 Figure Captions

Figure 1. a) Location of data in Canada Basin. Oceanic, transitional and continental crustal velocities from analysis of the sonobuoys are marked with white, green and black symbols, respectively. Thin solid black lines: coincident seismic reflection profiles. Yellow/cyan lines: assembled seismic transects shown in the paper. Dotted yellow line: Canada Basin Gravity Low (CBGL). Dotted red lines indicate basement depression. Also shown are previous crustal scale profiles: near Northwind Ridge (Jackson et al. 1995), near Alaskan margin (Baggeroer and Falconer, 1982; Mair & Lyons, 1981); and across Canadian Arctic margin (Stephenson et al., 1994 and Berry and Barr, 1971). b) Enlargment with sonobuoys labeled. Small labelled grey boxes indicate sonobuoys with undefined crustal type.

Figure 2. Idealized transects of (a) magma-rich (volcanic) passive margin showing the seaward dipping reflections (SDRs), and intruded/underplated body, modified from Blaich et al. (2011); and (b) magma-poor (non-volcanic) margin showing the exhumed continental mantle adjacent to oceanic crust, modified from Mohn et al. (2012). OCB: oceanic-continent boundary, OCT: ocean-continent transition zone. Velocities shown are values used in this paper.

Figure 3. Observed velocity/depth curves, excluding the sedimentary layers, determined from analyses of the wide angle reflection/refraction data (after Chian and Lebedeva-Ivanova, 2015) are plotted in three groups: a) continental, b) oceanic and c) transitional. The grey zone illustrates the range of velocities compiled for oceanic crust at age of 142-143 Ma in North Atlantic Ocean (after White et. al., 1992). The groupings are based on the velocity criteria shown in Table I.

Second row of boxes show the same curves as the first row but colored and sized for easier labelling.

Figure 4. Sonobuoy 0726, an example with oceanic crustal velocities, is displayed (for location see 726 in red in Figure 1). a) The reflection profile along the model. b) Same shots recorded by the sonobuoy, modelled and plotted by Reduced Normal Move-Out (NMO) transform such that each wide-angle reflection phase (dotted blue) at zero offset matches exactly with the corresponding event on the refection profile. Sedimentary velocities were modelled by Chian and Lebedeva-Ivanova (2015) and used for modelling deeper arrivals with labels indicating their corresponding velocities. Inset of b) shows crustal refraction phases picked (yellow bars) for statistical error analysis with results shown to its left; every trace is picked. c) 1D velocity/depth curve at the sonobuoy location. d) Final 2D velocity model from the forward modeling, with 5 sets of ray paths illustrated. Each model layer is parameterized by a linear vertical velocity gradient with no horizontal changes in velocity inside the same layer.

Figure 5. Sonobuoy 1034, an example with transitional crustal velocities, is displayed. See 1034 (in red) in Figure 1 for its location and Figure 4 for caption.

Figure 6. Sonobuoy 1003, an example with continental crustal velocities, is displayed. See 1003 (in red) in Figure 1 for location and Figure 4 for caption.

Figure 7. Magnetic anomaly map of Canada Basin (after Gaina et al., 2011). Sonobuoy models classified as oceanic are shown as white squares, continental as black squares and transitional as blue diamonds. Dashed polygon indicates ocean-continent boundary (OCB). The number of each solid blue line indicates the figure number of the seismic transects. D3 indicates a regional magnetic zone defined by Saltus et al., (2011). Parallel white dots indicate a basement depression.

Figure 8. Free Air gravity anomaly map of Canada Basin (with onshore Bouguer anomaly; after Andersen et al, 2010). Sonobuoy models classified as oceanic are shown as white squares, continental as black squares and transitional as blue diamonds. Dashed polygon indicates the ocean-continent boundary (OCB). The number of each solid blue line indicates the figure number of the seismic transects. Parallel red dots indicate a basement depression.

Figure 9. Seismic transect across the northernmost Canada Basin (see figure 1 for location). a) Observed magnetic and gravity anomalies (extracted from gridded maps in Figures 7 and 8; CBGL: Canada Basin gravity low. C|C indicates course change. b) Reflection profile (Hilbert transformed) converted to depth using a velocity model based on all available sonobuoy data along the transect; sonobuoy labels plotted on the seafloor; brackets indicate offline stations. The time-depth conversion process includes: assign distance to each trace of reflection profile, digitize seafloor and basement in time domain, and perform time-depth conversion assuming a compaction-oriented exponential velocity function for the sediments in central Canada Basin (region 3; Shimeld et al. 2016). Sonobuoy velocity models from the base of sedimentary section are overlain as solid lines and labels show their corresponding velocities in km/s. HVLC: High velocity lower crust. SDR: Seaward dipping reflectors. Final crustal model is constructed in the depth domain that in general matches all available sonobuoy data. The rectangular area marked on panel b) is enlarged in c) to show details (vertical exaggeration: 7.6:1). Vertical arrows indicate base of sedimentary layers.

Figure 10. Seismic transect across the central Canada Basin (see figure 1 for location). Top: magnetic (blue line) and gravity (red line) anomalies extracted from gridded data in Figures 7 and 8, with computed Free Air gravity anomaly (black line) for Moho constraint. Gravity computation used a velocity-density curve from Ludwig et al. (1970). Computed gravity is DC-shifted by -712 mGal

and assumes a constant density of 3.3 g/cm^3 underneath the model. Bottom: velocity model overlain by depth-converted reflection profile. Sonobuoy 1021 is indicated in blue to contrast with adjacent instruments. See Figure 9b for more description.

Figure 11. Seismic transect across southern Canada Basin (see Figure 1 for location). a) Magnetic (blue line) and gravity (red line) anomalies extracted from gridded data in Figures 7 and 8. C|C indicates course changes. b) Velocity model overlain by depth-converted reflection profile. Sonobuoy 804 is indicated in blue to contrast with adjacent instruments. The rectangular area marked on panel b) is enlarged in c) to show details of deeper reflectors coincident with 7.4 km/s layer (vertical exaggeration: 11:1). See Figure 9b for more description.

Figure 12. Seismic transect from Alaskan margin northward to nearly parallel to Canada Basin Gravity Low (CBGL). Top: magnetic (blue line) and gravity (red line) anomalies extracted from gridded data in Figures 7 and 8. Bottom: the transect combines 4 seismic profiles, crosses continental, transitional and oceanic crust, and shows distinctive features in crustal velocity structures as well as basement morphology. Reflection profiles are brute stack data converted to depth, with positive amplitudes plotted as grey and negative amplitudes as blue. See figures 9a and 9b for more description.

Figure 13. Seismic reflection profile that overlaps the refraction lines reported in Mair and Lyons (1981). The velocities reported by them are plotted in red and the velocities based on our sonobuoy data are in black. Sonobuoy 1002 is categorized as in transitional zone due to an observation of HVLC. But this region is in general continental because: crustal velocity are in the continental range; crust shows consistent reflection characters with regional rotated fault blocks; and it is surrounded by typical continental crust in the vicinity of the shelf.

Figure 14. Seismic reflection profile that overlaps the refraction lines reported in Baggeroer and Falconer (1982). The velocities reported by them are shown in red and labeled CANBARX 78.

Figure 15. Interpreted distribution of crustal regions plotted on a) bathymetric, b) gravity and c) magnetic maps (for colour bars of scale see Figures 1, 8 and 7). The regions are based on the combination of sonobuoy velocities, magnetic and gravity data, seismic reflection control and geological context. The area with gray shading is the ocean-continent transition. Its inner limit is the ocean-continent boundary. The star shows the position of sonobuoy 1013. The red and yellow dots indicate the position of the Baggeroer and Falconer (1982) and Jackson et al. (1995) refraction experiments. Abbreviations: CBGL-N is Canada Basin Gravity Low-North, CBGL-S is Canada Basin Gravity Low-South, MR is Magma Rich, MP is Magma Poor, HALIP is High Arctic Large Igneous Province.

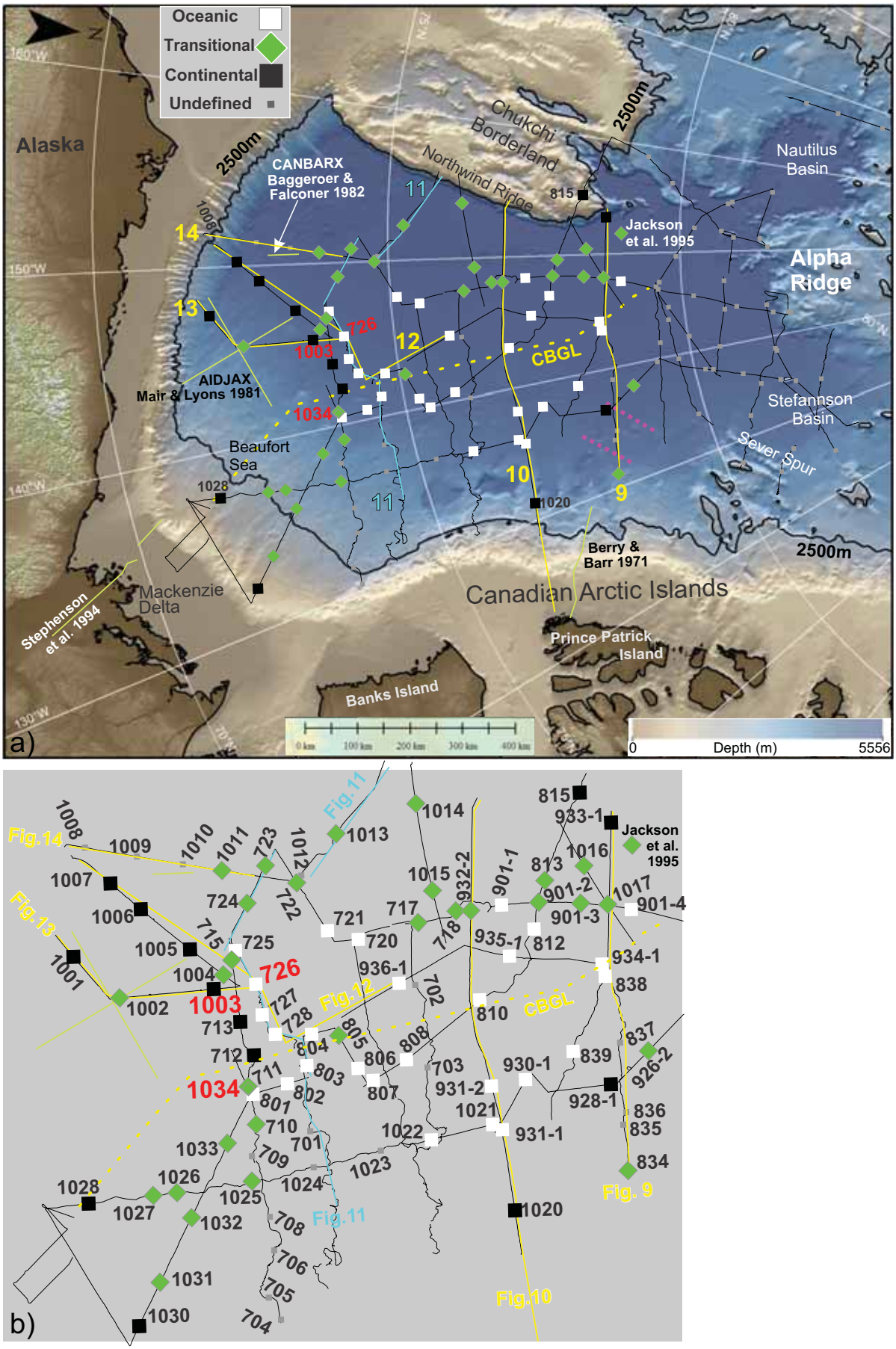

Figure 1. a) Location of data in Canada Basin. Oceanic, transitional and continental crustal velocities from analysis of sonobuoys are marked with white, green and black symbols, respectively. Thin solid black lines: coincident seismic reflection profiles. Yellow/cyan lines: assembled seismic transects shown in paper. Dotted yellow line: Canada Basin Gravity Low (CBGL). Dotted red lines indicate basement depression. Also shown are previous crustal scale profiles: near Northwind Ridge (Jackson et al., 1995), near Alaskan margin (Baggeroer & Falconer, 1982; Mair & Lyons, 1981); and across Canadian Arctic margin (Stephenson et al., 1994; Berry & Barr, 1971). b) Enlargment with sonobuoys labelled. Small labelled grey boxes indicate sonobuoys with undefined crustal type.

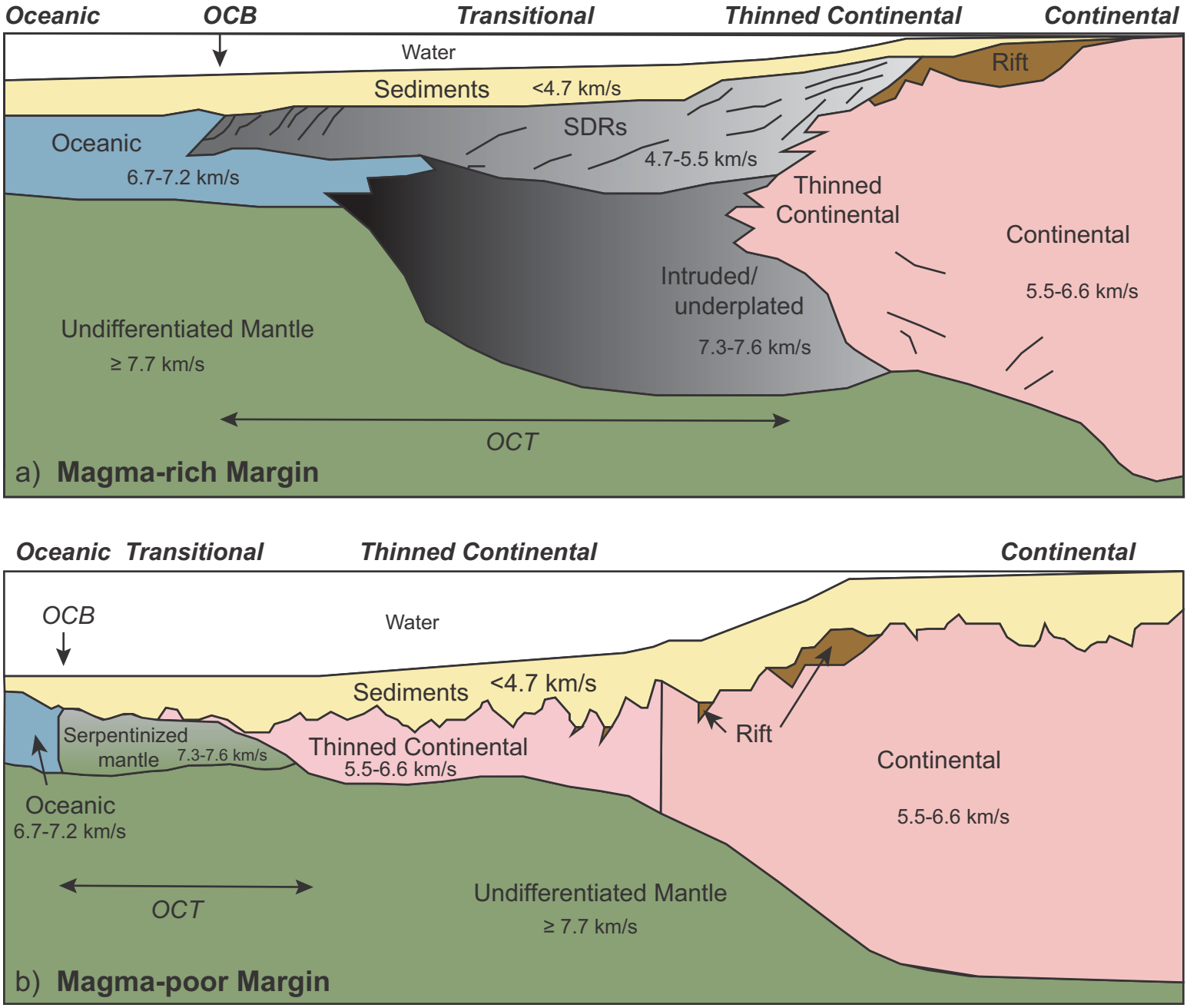

Figure 2. Idealized transects of a) magma-rich (volcanic) passive margin showing seaward dipping reflections (SDRs), and intruded/underplated body, modified from Blaich et al. (2011); and b) magma-poor (non-volcanic) margin showing exhumed continental mantle adjacent to oceanic crust, modified from Mohn et al. (2012). OCB: oceanic-continent boundary, OCT: ocean-continent transition zone. Velocities shown are values used in this paper.

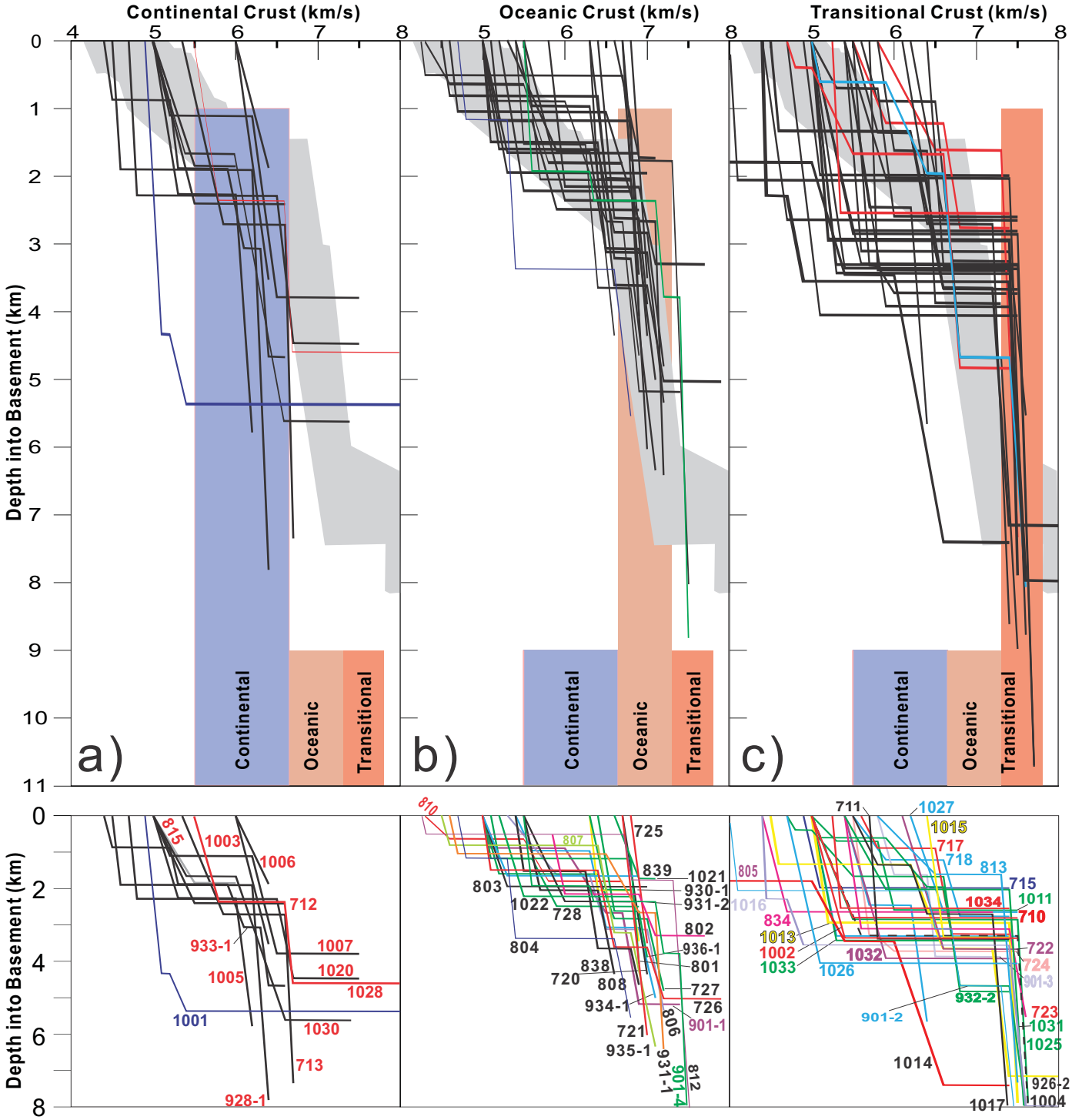

Figure 3. Observed velocity/depth curves, excluding sedimentary layers, determined from analyses of wide angle reflection/refraction data (after Chian and Lebedeva-Ivanova, 2015) are plotted in three groups: a) continental, b) oceanic and c) transitional. The grey zone illustrates the range of velocities compiled for oceanic crust at age of 142-143 Ma in North Atlantic Ocean (after White et. al., 1992). The groupings are based on the velocity criteria shown in Table 1. Second row of boxes show the same curves as the first row but colored and sized for easier labelling.

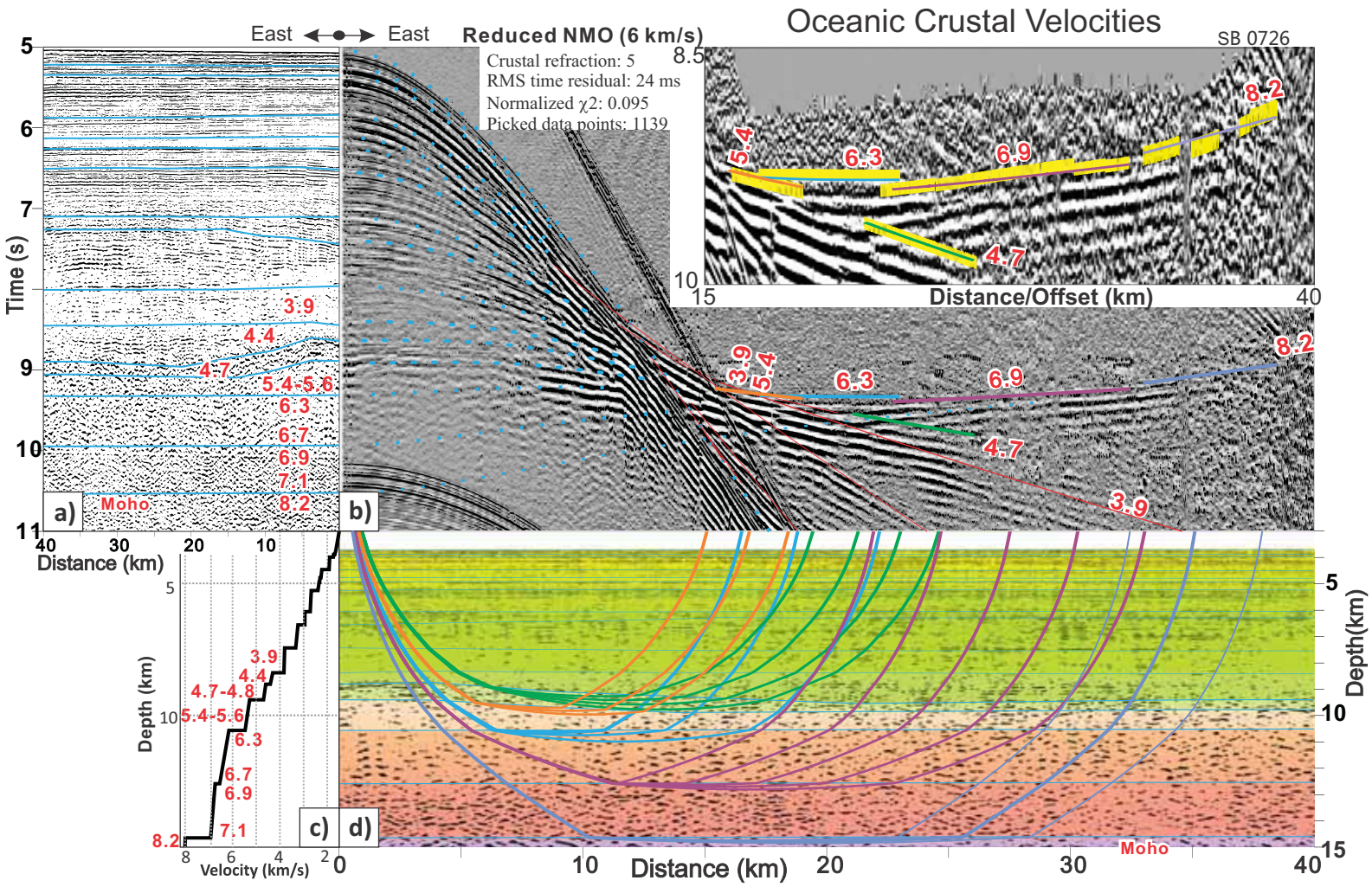

Figure 4. Sonobuoy 0726, an example with oceanic crustal velocities, is displayed (for location see 726 in red in Figure 1). a) Reflection profile along the model. b) Same shots recorded by the sonobuoy, modelled and plotted by Reduced Normal Move-Out (NMO) transform such that each wide-angle reflection phase (dotted blue) at zero offset matches exactly with the corresponding event on refection profile. Sedimentary velocities were modelled by Chian and Lebedeva-Ivanova (2015) and used for modelling deeper arrivals with labels indicating their corresponding velocities. Inset of b) shows crustal refraction phases picked (yellow bars) for statistical error analysis with results shown to its left; every trace is picked. c) 1D velocity/depth curve at sonobuoy location. d) Final 2D velocity model from forward modeling, with 5 sets of ray paths illustrated. Each model layer is parameterized by a linear vertical velocity gradient with no horizontal changes in velocity inside the same layer.

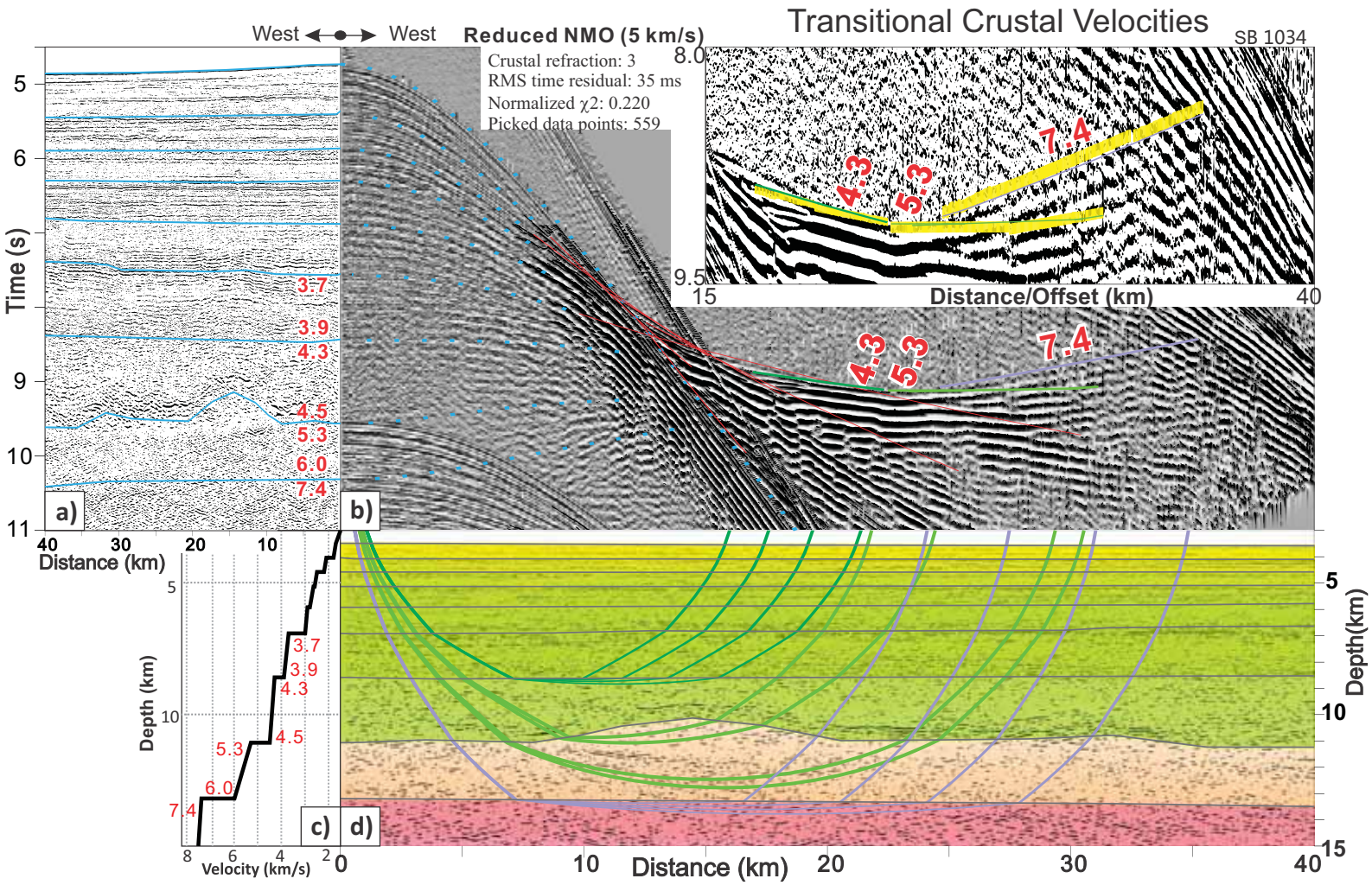

Figure 5. Sonobuoy 1034, an example with transitional crustal velocities, is displayed. See 1034 (in red) in Figure 1 for its location and Figure 4 for caption.

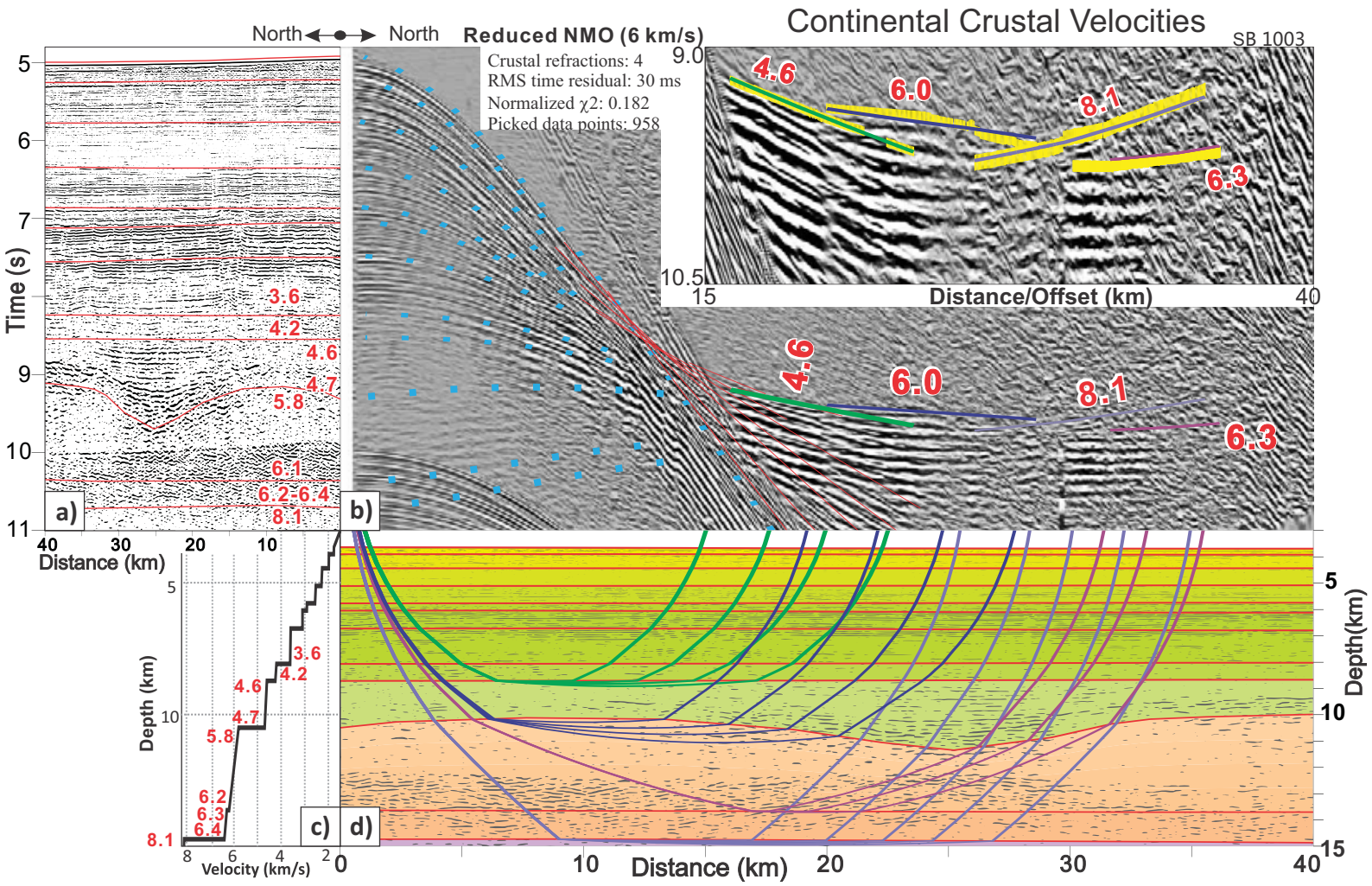

Figure 6. Sonobuoy 1003, an example with continental crustal velocities, is displayed. See 1003 (in red) in Figure 1 for location and Figure 4 for caption.

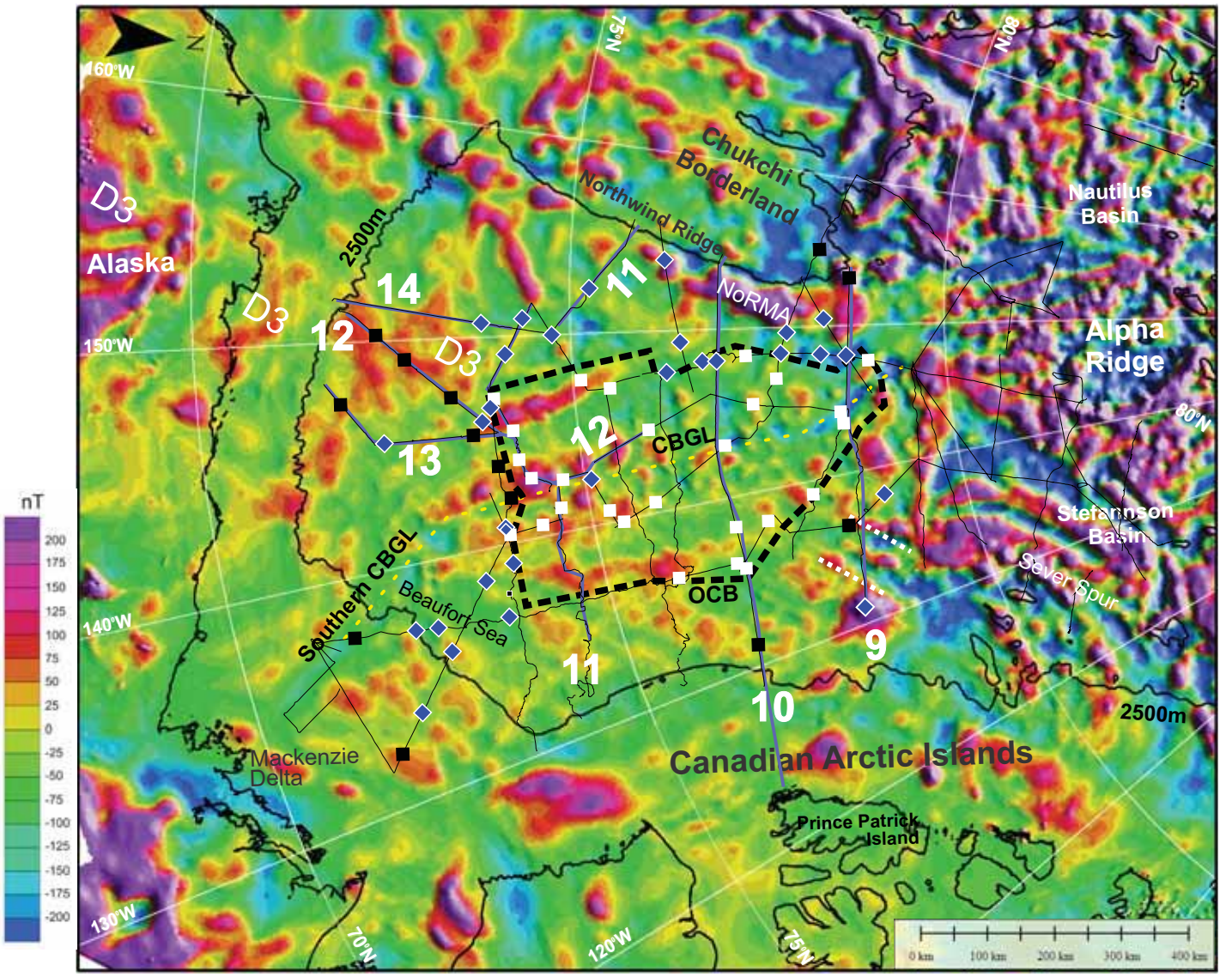

Figure 7. Magnetic anomaly map of Canada Basin (after Gaina et al., 2011). Sonobuoy models classified as oceanic are shown as white squares, continental as black squares and transitional as blue diamonds. Dashed polygon indicates ocean-continent boundary (OCB). The number of each solid blue line indicates figure number of seismic transects. D3 indicates a regional magnetic zone defined by Saltus et al., (2011). Parallel white dots indicate a basement depression.

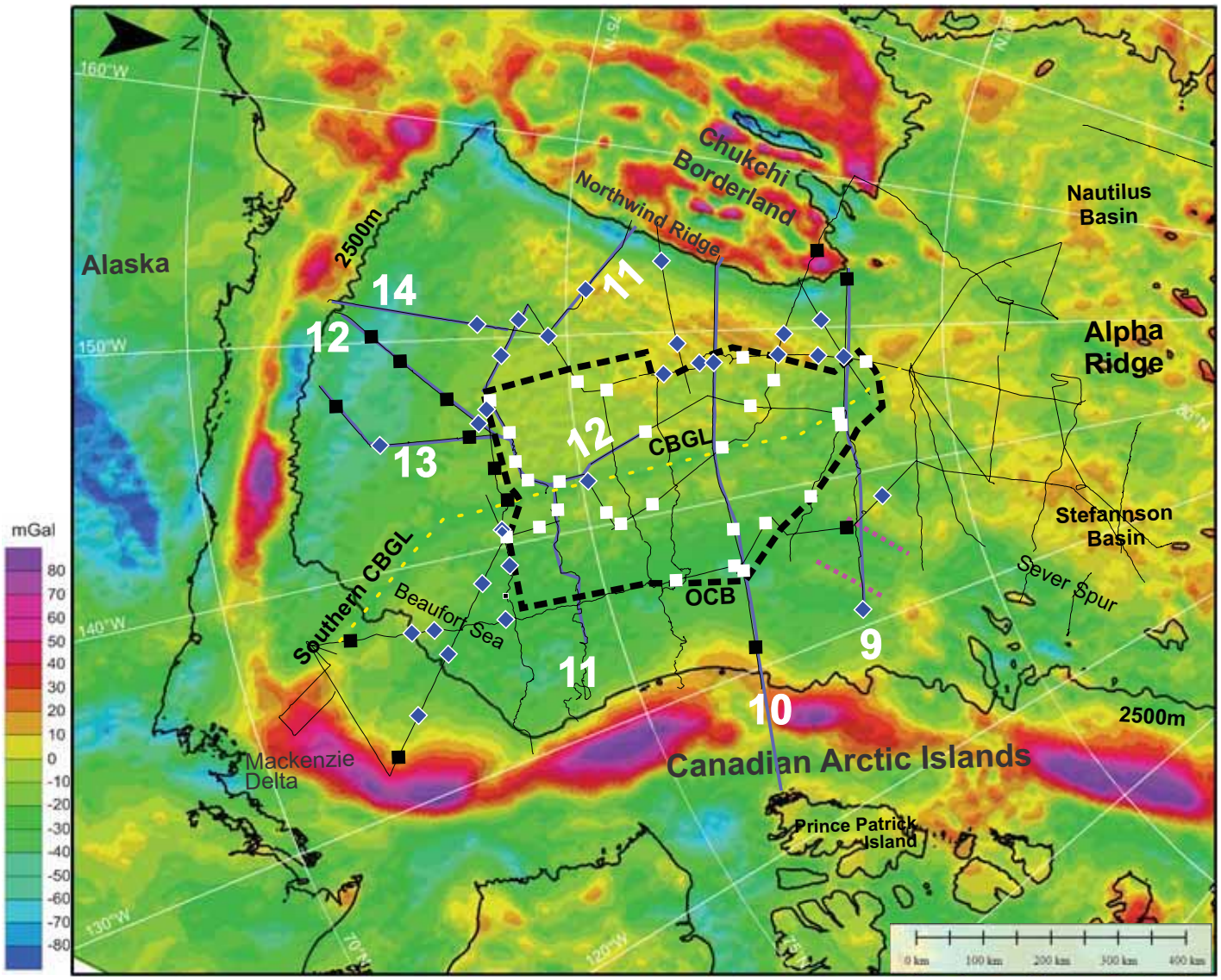

Figure 8. Free Air gravity anomaly map of Canada Basin (with onshore Bouguer anomaly; after Andersen et al., 2010). Sonobuoy models classified as oceanic are shown as white squares, continental as black squares and transitional as blue diamonds. Dashed polygon indicates ocean-continent boundary (OCB). The number of each solid blue line indicates figure number of seismic transects. Parallel red dots indicate a basement depression.

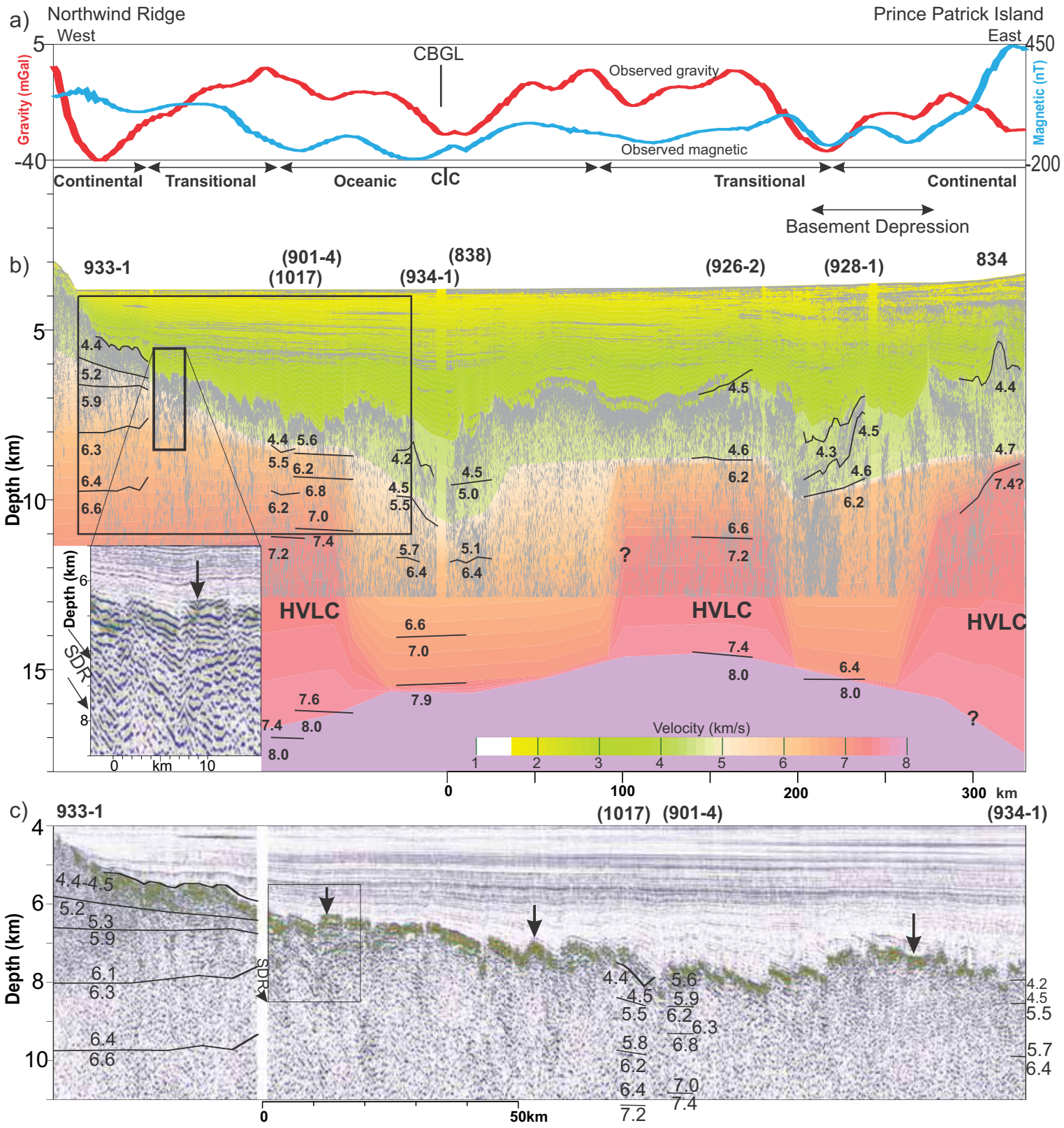

Figure 9. Seismic transect across northernmost Canada Basin. a) Observed magnetic and gravity anomalies (extracted from gridded maps in Figures 7 and 8; CBGL: Canada Basin gravity low. C|C indicates course change. b) Reflection profile (Hilbert transformed) converted to depth using a velocity model based on all available sonobuoy data along transect; sonobuoy labels are plotted on seafloor; brackets indicate offline stations. The time-depth conversion process includes: assign distance to each trace of reflection profile, digitize seafloor and basement in time domain, and perform time-depth conversion assuming a compaction-oriented exponential velocity function for sediments in central Canada Basin (region 3; Shimeld et al. 2016). Crustal velocity models are overlain as solid lines and labels show their corresponding velocities in km/s. HVLC: High velocity lower crust. SDR: Seaward dipping reflectors. Final crustal model is constructed in depth domain that in general matches all available sonobuoy data. The rectangular area marked on panel b) is enlarged in c) to show details (vertical exaggeration: 7.6:1). Vertical arrows indicate sedimentary base.

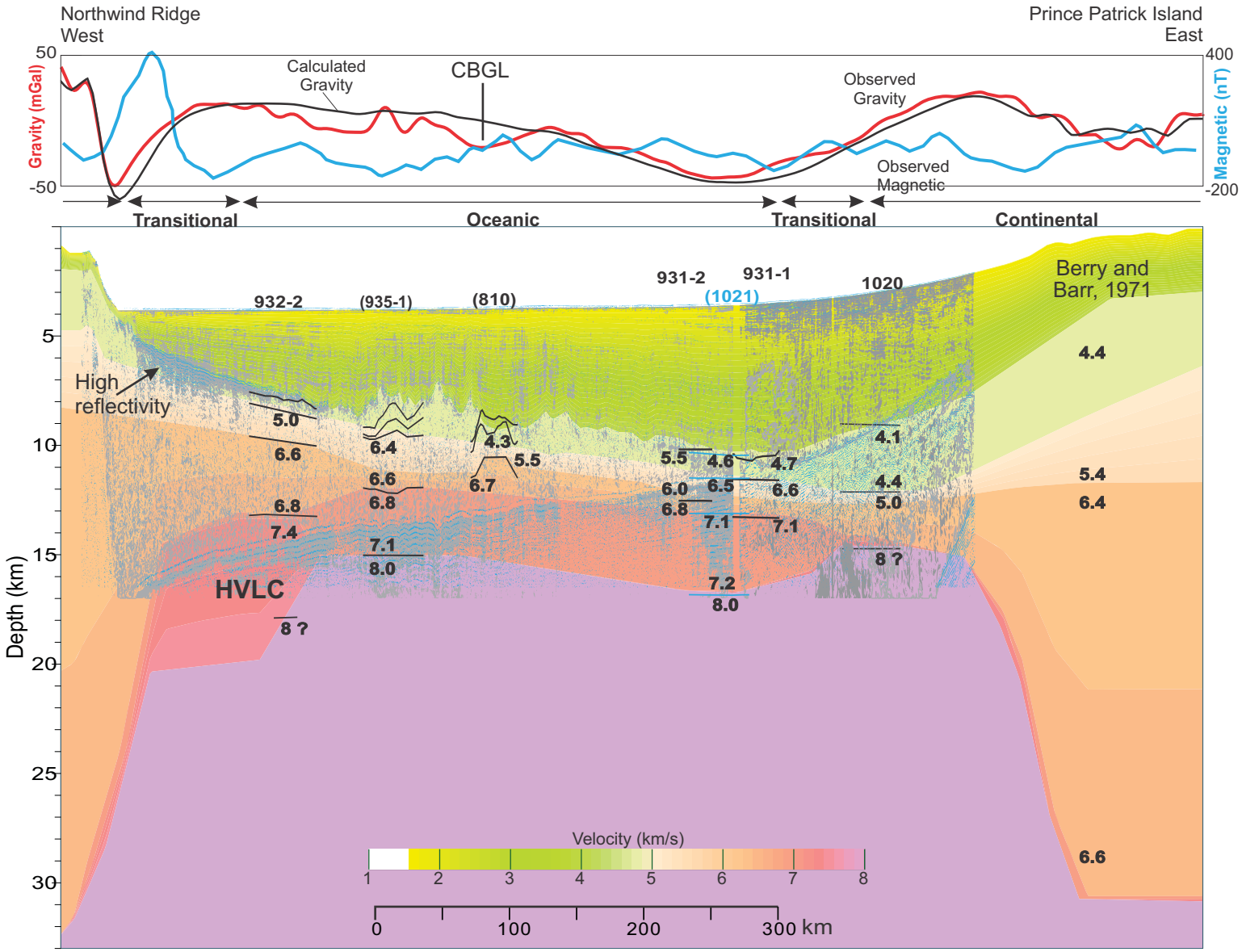

Figure 10. Seismic transect across central Canada Basin (see figure 1 for location). Top: magnetic (blue line) and gravity (red line) anomalies extracted from gridded data in Figures 7 and 8, with computed Free Air gravity anomaly (black line) for Moho constraint. Gravity computation used a velocity-density curve from Ludwig et al. (1970). Computed gravity is DC-shifted by -712 mGal and assumes a constant density of 3.3 g/cm3 underneath the model. Bottom: velocity model overlain by depth-converted reflection profile. Sonobuoy 1021 is indicated in blue to contrast with adjacent instruments. See Figure 9b for more description.

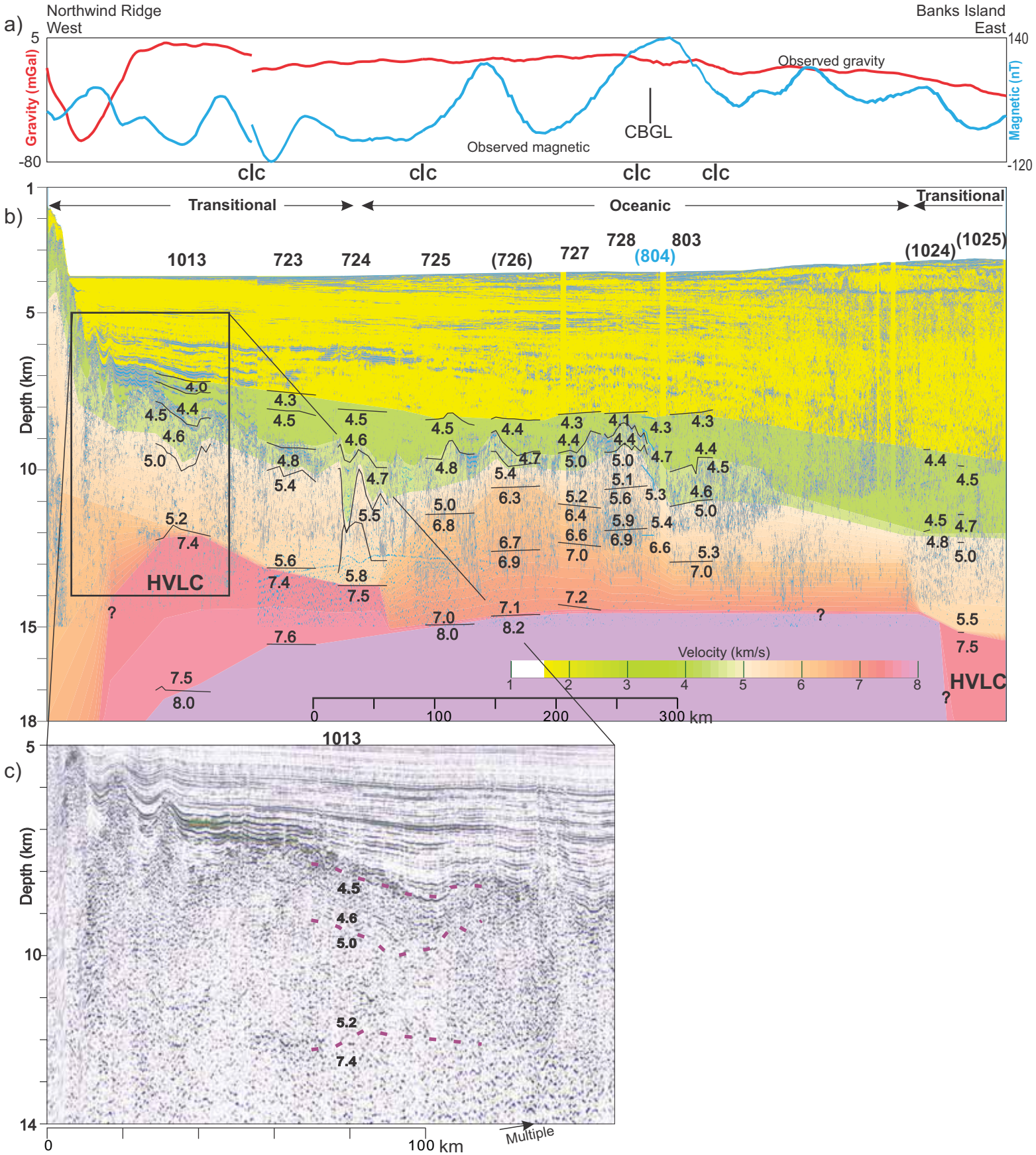

Figure 11. Seismic transect across southern Canada Basin (see Figure 1 for location). a) Magnetic (blue line) and gravity (red line) anomalies extracted from gridded data in Figures 7 and 8. C|C indicates course changes. b) Velocity model overlain by depth-converted reflection profile. Sonobuoy 804 is indicated in blue to contrast with adjacent instruments. The rectangular area marked on panel b) is enlarged in c) to show details of deeper reflectors coincident with 7.4 km/s layer (vertical exaggeration: 11:1). See Figure 9b for more description.

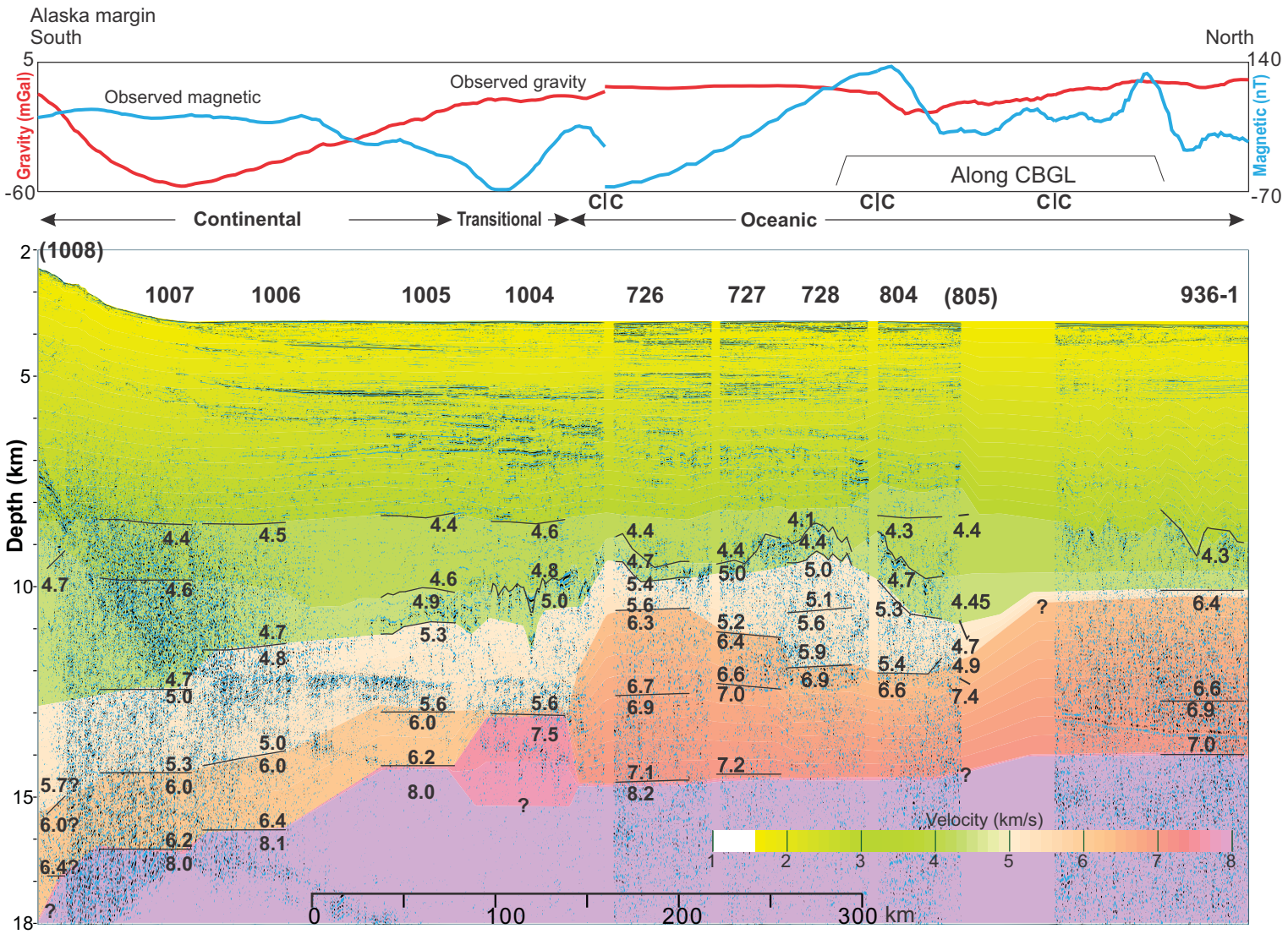

Figure 12. Seismic transect from Alaskan margin northward to nearly parallel to Canada Basin Gravity Low (CBGL). Top: magnetic (blue line) and gravity (red line) anomalies extracted from gridded data in Figures 7 and 8. Bottom: the transect combines 4 seismic profiles, crosses continental, transitional and oceanic crust, and shows distinctive features in crustal velocity structures as well as basement morphology. Reflection profiles are brute stack data converted to depth, with positive amplitudes plotted as grey and negative amplitudes as blue. See Figures 9a and 9b for more description.

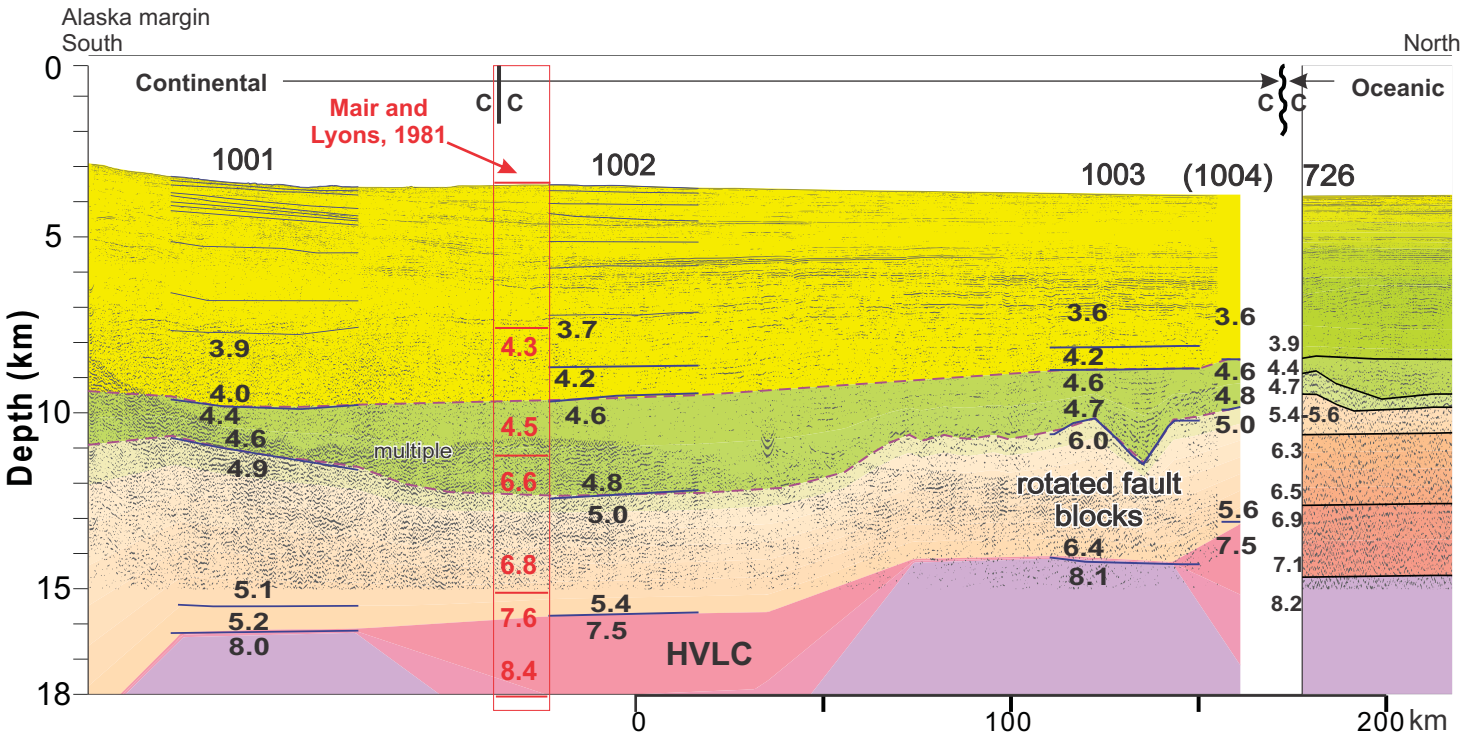

Figure 13. Seismic reflection profile that overlaps the refraction lines reported in Mair and Lyons (1981). The velocities reported by them are plotted in red and the velocities based on our sonobuoy data are in black. HVLC: high velocity lower crust. Sonobuoy 1002 is categorized as in transitional zone due to an observation of HVLC. But this region is in general continental because: crustal velocity is in the continental range; crust shows consistent reflection characters with regionally rotated fault blocks; and it is surrounded by typical continental crust in the vicinity of the shelf.

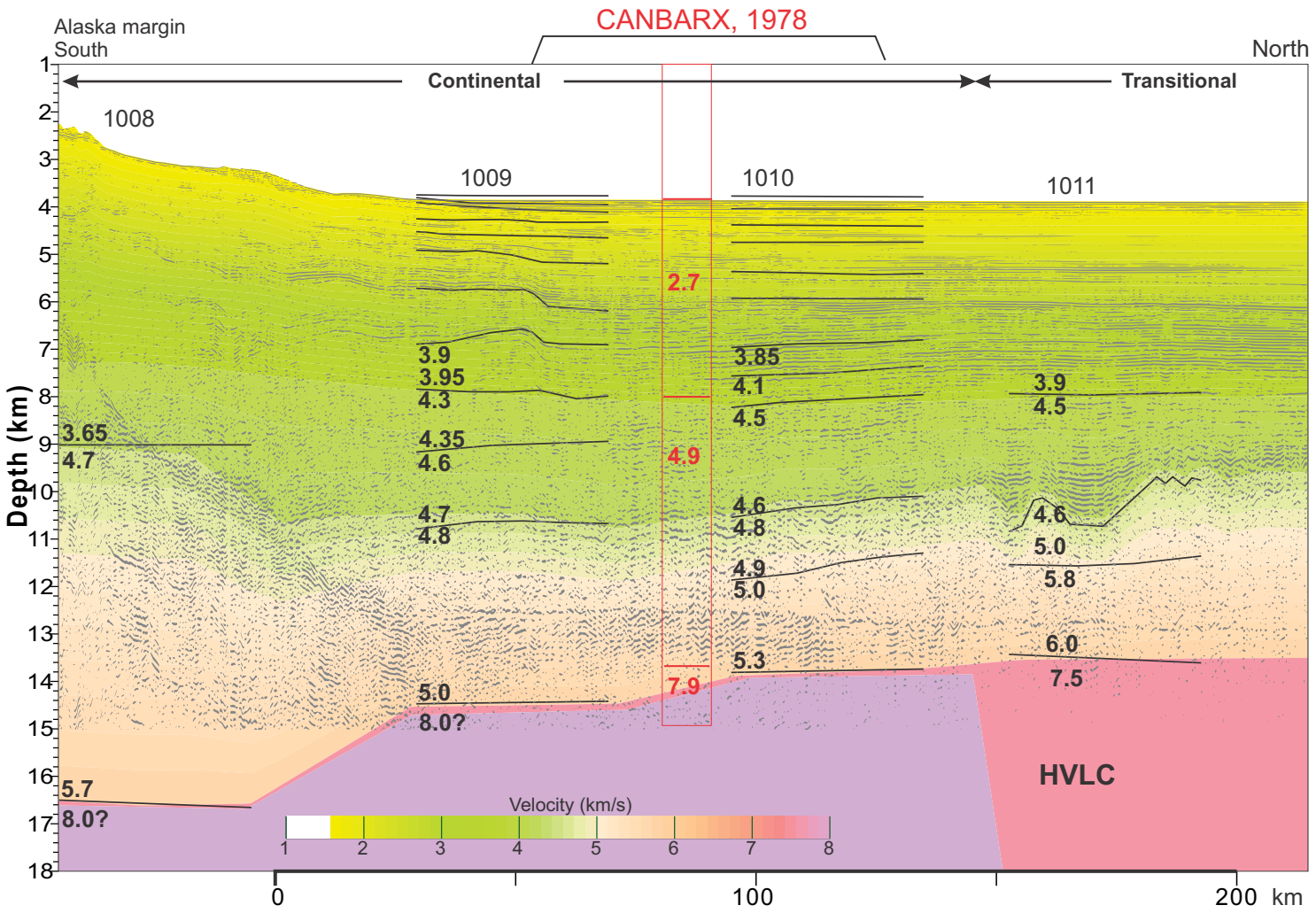

Figure 14. Previous refraction lines reported in Baggeroer and Falconer (1982) projected onto an adjacent profile of ours with sonobuoy results. Meaningful velocities reported by them are shown in red and labeled as CANBARX 78. See text for comparisons and interpretations.

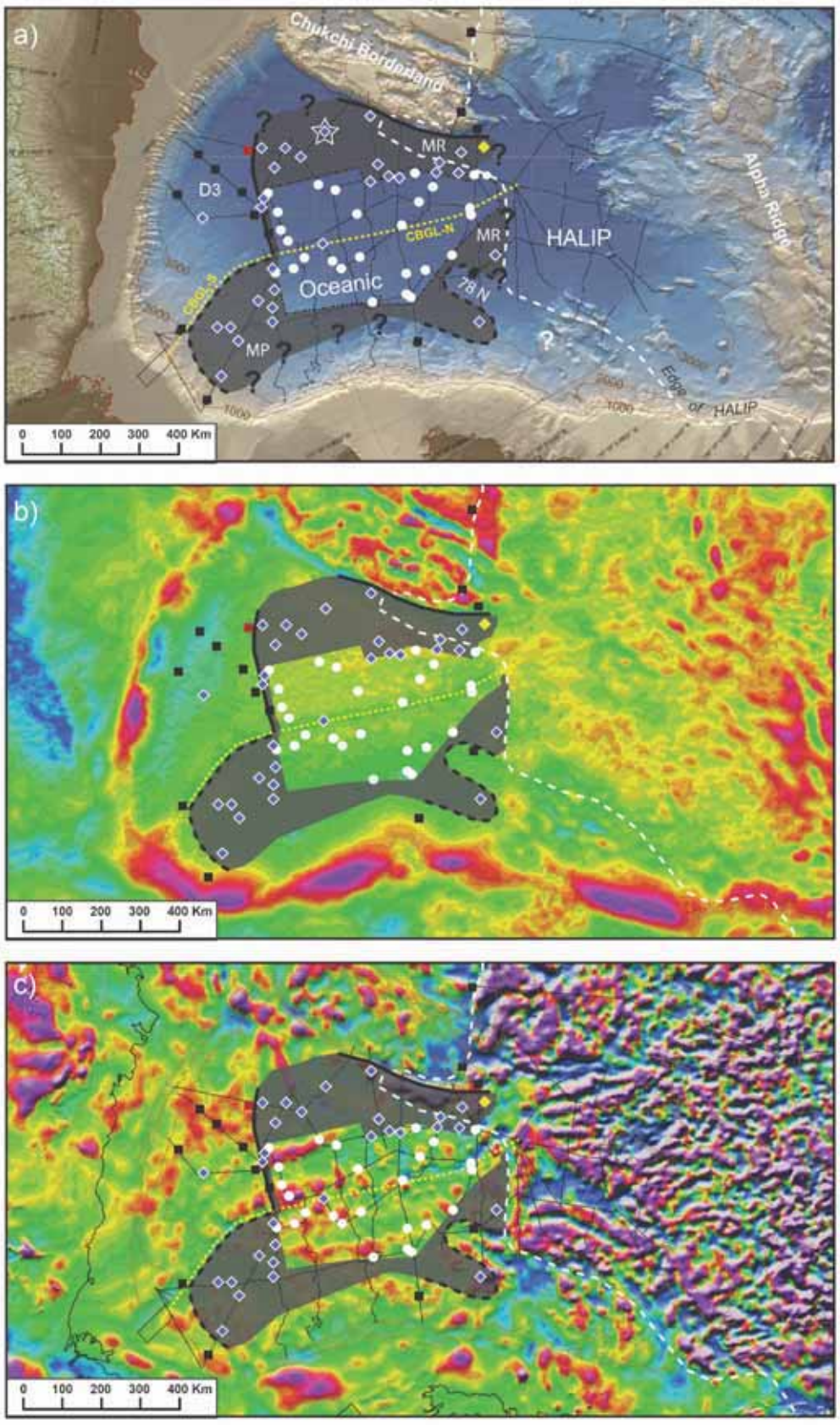

Figure 15. Interpreted distribution of crustal regions plotted on a) bathymetric, b) gravity and c) magnetic maps (for colour bars of scale see Figures 1, 8 and 7). The regions are based on combination of sonobuoy velocities, magnetic and gravity data, seismic reflection control and geological context. The area with gray shading is the ocean-continent transition. Its inner limit is the ocean-continent boundary. Star shows the position of sonobuoy 1013. Red and yellow dots indicate positions of refraction experiments by Baggeroer and Falconer (1982) and Jackson et al. (1995). CBGL-N: Canada Basin Gravity Low-North; CBGL-S: Canada Basin Gravity Low-South; MR: Magma Rich; MP: Magma Poor; HALIP: High Arctic Large Igneous Province.